SYNTHESIS OF CROWN ETHER/AMMONIUM SALT FOR ELECTRON TRANSFER STUDY.

Dong Han, M. Sc.

Thesis Prepared for the Degree of

MASTER OF SCIENCE

UNIVERSITY OF NORTH TEXAS

May 2002

APPROVED:

David J. Wiedenfeld, Major Professor.
Robert Desiderato, Committee Member.
Michael Richmond, Chair of Graduate Studies in the Department of Chemistry
Ruthanne Thomas, Chair of the Department of Chemistry
C. Neal Tate, Dean of the Robert B. Toulouse School of Graduate Studies

Han, Dong. Synthesis of Crown Ether/Ammonium Salt for Electron Transfer Study. Master of Science (Chemistry), May 2002, 58 pp., 1 table, 4 illustrations, 52 references.

The theoretical model of Beratan and Onuchic predicts a large attenuation of ET rates through hydrogen bonds; however, the effect of individual hydrogen bond on electron transfer reaction has not been systematically studied. The organic complexes in this study are a series of crown ether / ammonium salt, which incorporate a redox partner on each component of the complex. The dimethoxynaphthalene redox donor was attached to the crown ether and a series of ammonium salts was synthesized which bear substituted quinone and naphthoquinone acceptor. The complexes characterization and preliminary electron transfer rate measurement were completed with UV/Vis and steady-state emission spectroscopy.

ACKNOWLEDGMENTS

I thank the Robert A. Welch Foundation (Grant# B-1415), the ACS-Petroleum Research Fund (Grant# 33245-G4) and University of North Texas for financial support.

TABLE OF CONTENTS

LIST OF TABLES

Table Page

LIST OF ILLUSTRATIONS

Figure Page

I. INTRODUCTION

Long-distance electron transfer (ET) between two redox centers may be defined as those processes in which the electron transfer takes place over distances substantially larger than the sum of the van der Waals radii of those centers. [1] In this case, the direct overlap between the localized donor and acceptor wave functions is not important. This analysis might lead one to conclude that long-distance ET processes are very slow and inefficient. But, many reported examples exist to demonstrate that long-range ET processes occur over large distances at lightening speeds and with very high efficiency. [2]

Long-distance electron-transfer reactions are essential and ubiquitous phenomena in biological systems such as the photosynthetic and respiratory electron-transfer chains and also in many simple chemical reactions.[3,4] The importance and complexity of electron-transfer reactions in nature have led many scientists to look for ways to study the fundamental chemistry of these processes in simplified model systems. There have been many studies of ET reactions through saturated organic systems [5-7] and protein-based systems [8,9] to probe the mechanism of this important process.

When the electron transfer proceeds directly from the edge of the donor to the edge of the acceptor by a mechanism not involving the orbitals of the bridge molecule, it is referred to as a through-space pathway. If, on the other hand, the orbitals of the bridge group assist in carrying the charge transfer between the donor and the acceptor, the pathway is referred as a through-

bond pathway and coupling between the donor and acceptor is therefore achieved through the orbitals of the bridging groups. [10,11]

Studies of ET through rigid saturated hydrocarbon spacers have shown that intramolecular ET is dramatically faster than intermolecular (through vacuum) ET at the same distances. Results from protein based systems also indicate that through-bond ET is favored over through-space, even though analyses are hampered by the fact that proteins frequently contain numerous potential ET pathways. Generally, a hydrogen bond is implicated as being part of the ET pathway.

The study of electron transfer reactions, wherein the donor and acceptor are assembled by hydrogen bonding interactions, has attracted considerable interest in recent years.[12,13] These studies are very important because of their direct relevance to the studies of electron transfer in biological systems. For example, in the case of protein electron transfer, electronic coupling through hydrogen bonds is extremely important due to the prevalence of hydrogen bond networks in proteins. Because of the directionality of hydrogen bonds it is possible to know the separation and relative orientation of the components in hydrogen bonded systems. Hence hydrogen bonded systems provide an attractive alternative to covalently linked systems for the study of electron transfer reactions. Although some reports dealing with studies of electron transfer reactions in hydrogen bonded systems are available, systematic studies about the effect of factors such as driving force, distance, etc. on the rate of electron transfer in such systems are absent. It is still not clear whether hydrogen bonds provide better or worse electronic coupling pathways than the widely studied covalent linkages, and both views have their loyal supporters. One report suggests that hydrogen bond mediated ET is somewhat slower than covalent bond

mediated ET as is suggested by theory; the other report is very surprising as the electronic coupling modulated by a hydrogen-bond interface was reported to be greater than that of a carbon-carbon sigma-bond interface! [14] Clearly systematic studies of the effect of hydrogen bonds on ET rate are necessary. Beratan and Onuchic [15] have developed a theoretical model for predicting the ET pathways in proteins. They predict that the transfer through bonds will be greatly preferred to through-space transfer. In this model, the effect of a hydrogen bond on the ET rate is comparable to that of three normal covalent bonds.

A research program was initiated to systematically study the effects of hydrogen bonds on the rate of electron transfer. My contribution to this project was: (1) syntheses of a series of supramolecular complexes that consist of a redox donor/acceptor partner rigidly attached to the crown ether derivatives and another redox partner rigidly attached to ammonium salt derivatives without hydrocarbon spacers incorporated in between the redox partner and appropriate partner of the hydrogen bonding assembly. (2) measurement of electron transfer rate constants under various conditions.

I.1 Basic Electron Transfer Theory

A brief discussion of electron transfer is presented in the following section.

Equations shown below represent the system in which we are interested here.

$D^* - Sp - A \rightarrow D^+ - Sp - A^-$ (1)

$D^- - Sp - A \rightarrow D - Sp - A^-$ (2)

Where D stands for the donor, Sp for spacer, and A for acceptor.

Marcus gives the rate constant, k, of the electron transfer in terms of a free energy of activation ΔG^* for the reaction: [16,17]

$$k = \rho(r) \; Z \exp(- \Delta G^* / RT) \qquad (3)$$

Where $\rho(r)$ is the probability for the electron transfer to occur normalized to the number of times the molecules acquired the correct nuclear configuration to pass through the intersection of the potential energy surfaces of the reactants and products. Z is either the collision frequency in a bimolecular reaction or the vibrational frequency in an intramolecular reaction. According to this semiclassical theory, k is governed by three parameters: (1) the electron coupling between reactants and products, (2) the free-energy change for the reaction ($\Delta G°$), and (3) the total reorganization energy (λ), the latter including both inner-sphere (λ_I) and solvent (λs) contributions. Thus the rates are predicted to increase to a maximal value and then decrease as the driving force increases further; the region of increasing ET rates is commonly referred to as "normal," while the surprising region of falling ET rates has been coined "inverted." The inverted driving-force effects arise in the semiclassical formulation by a reduction of the Frank-Condon barrier for ET as $-\Delta G^0$ increases beyond the value of λ. In most cases, driving force dependence data are better fit by treatments that include quantum effects; typically, the inverted effect is attenuated compared to predictions based on equation (4) due to nuclear tunneling.

$$k = 4\Pi^2 H^2_{AB} \exp[-(\Delta G° + \lambda)^2 / 4\lambda RT] / \{h * (4\Pi\lambda RT)^{1/2}\} \qquad (4)$$

Where h is the Plank constant, H_{AB} is the electron coupling between reactants and products.

Early tests on this theory were unsuccessful and few cases seemed to show the inverted region. This variance was thought to be mainly due to four reasons: [18,19] first, intermolecular reactions were selected to simulate intramolecular ones and the interaction of the reactants depended on diffusion instead of molecular structure; second, very exoergic reactions were chosen, which allowed product formation in the excited states to give artificially high rates; third, extra reaction channels other than electron transfer presents; fourth, a true homogeneous series of donors and acceptors lacks. Recent studies [20,21] have corrected those deviations and shown an inverted region. Marcus predicts that the rate of electron transfer will depend strongly on the distance regime, as well as the dielectric properties of the medium.

The rate of electron transfer reactions can be strongly influenced by the nature of the medium intervening between the donor and the acceptor. These species may be solvent molecules or a molecular bridge, components of a supramolecular assembly, such as the protein matrix which envelops the photosynthetic reaction center.

Empirically, the dependence of electron transfer rate constant on donor-acceptor distance in a specified solvent takes on the form given by the equation (5):

$$k = k_0 \exp[-\alpha (r - r_0)] \qquad (5)$$

Where r is the donor-acceptor distance, r_0 is the distance usually van der Waals contact, at which the largest rate occurs, and α is a constant.

Electrons need not transfer from a donor to an acceptor via the direct overlap of their respective electronic wave functions. The molecule that resides between the donor and the acceptor may influence the rate of donor-acceptor electron transfer by means mixing their electronic states with those of the donor and acceptor. In the case where the donor and acceptor are covalently-linked, this consideration becomes especially important. Several virtual states of the spacer molecule may contribute to the overall electronic configuration of the donor-acceptor system. The degree to which each of these virtual states contributes to each the overall electronic structure of the system is determined by the magnitude of the electron exchange interaction involving these configurations. These concepts have come to be known as "superexchange." Kuznetzov and Ulstrup [22] considered the effect of spacer states which lie both higher and lower than the initial and final donor-acceptor states on the electron transfer rate. They found that the preexponential in the rate expression for electron transfer will decrease by a power law as the energy gap between the higher energy of bridge states and that of the initial state increases. Recent calculations by Larsson [23] and by Beratan [24] have shown that the participation of high-energy intermediate states of the bridging molecules dominate the electron transfer matrix elements for a variety of systems containing either complete-saturated or partially-saturated bridges.

The magnitude of the superexchange contribution to the total donor-acceptor electronic coupling will be proportional to both donor-acceptor orbital overlap and the overlap of orbitals of the

spacer with those on the donor and the acceptor and inversely proportional to the energy gap between the initial donor-acceptor state and the virtual state involving the spacer. A through-space interaction involves only direct overlap of the wave functions of the donor with those of the acceptor. On the other hand, the though-bond interaction involves participation of the wave function of the spacer molecules between the donor and acceptor.

I.2 Rate Measurement Techniques

Standard methods have been used for the kinetics measurements.[7] Two fluorescence-based techniques are primarily used. In the first, absolute fluorescence quantum yields are determined and used to infer electron transfer rates. In the second, time-resolved measurements of fluorescence quenching of the excited dimethoxynaphthalene are made. In the following section a short discussion about these two techniques is presented.

Fluorescence measurements can be broadly classified into two types of measurements, steady-state and time-resolved. Steady-state measurements are those performed with constant illumination and observation. The sample is illuminated with a continuous beam of light, and the intensity or emission spectrum is recorded. When the sample is first exposed to light, a steady state is reached almost immediately. Time-resolved measurement is used for measuring intensity decays or anisotropy decays. For these measurements, the sample is exposed to a pulse of light, where the pulse width is typically shorter than the decay time of the sample. It is very important to know that there is a rather simple relationship between steady-state and time-resolved measurements. The steady-state observation is simply an average of the time-resolved

phenomena over the intensity decay of the sample. During the time-averaging process, much of the molecular information available from fluorescence is lost. And the intensity decays also contain information that is lost during that process. In the case of energy transfer study by time-resolved fluorescence, the intensity decays reveal how acceptors are distributed in space around donors.

The quantum yield is the number of emitted photons relative to the number of absorbed photons. The lifetime determines the time available for the fluorophore to interact with or diffuse in its environment.

The meaning of the quantum yield and lifetime is best represented by a simplified Jablonski diagram (Figure 1). In this diagram, we focus attention on those processes responsible for return to the ground state. In particular, we are interested in the emission rate of the fluorophore (Γ) and its rate of nonradiative decay to S_0 (k_{nr}).

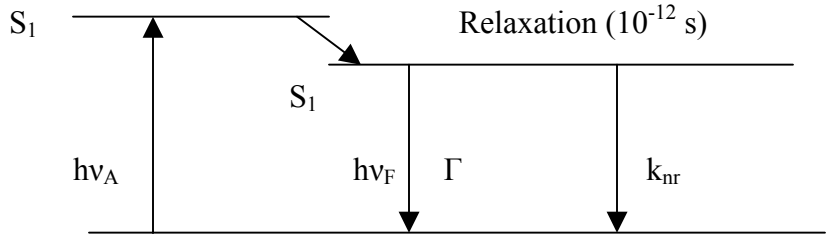

Figure 1. A simplified Jablonski diagram

The fluorescence quantum yield is the ratio of the number of photons emitted to the number absorbed. The processes governed by the rate constants Γ and k_{nr} both depopulate the excited state. Hence, the quantum yield is given by:

$$Q = \Gamma / (\Gamma + k_{nr}) \qquad (6)$$

For convenience, we have grouped all possible nonradiative decay processes with the single rate constant k_{nr}.

Lifetime of the excited state is prior to return to the ground state. Generally, fluorescence lifetimes are near 10 ns. The lifetime is given by

$$\tau = 1 / (\Gamma + k_{nr}) \qquad (7)$$

The lifetime is an average value of the time spent in the excited state. Once the quantum yield is obtained, the rate constant Γ can be inferred from that information.

Fluorescence resonance energy transfer is transfer of the excited-state energy from the initially excited donor (D) to an acceptor (A). The donor molecules typically emit at shorter wavelengths with overlap with the absorption spectrum of the acceptor. Energy transfer occurs without the acceptance of a photon and is the result of long-range dipole-dipole interactions between the donor and acceptor. The distance dependence of RET has resulted in its widespread use to measure distances between donors and acceptors.

The most common application of RET is to measure the distance between two sites on a macromolecule. If the D-A distance does not change during the excited-state lifetime, it can be determined from the efficiency of the energy transfer. The transfer efficiency can be determined by steady-state measurements of the extent of donor quenching due to the acceptor.

An important characteristic of energy transfer is that it occurs over distances comparable to dimensions of biological macromolecules. The distance at which RET is 50% efficient, called the Froster distance, [5] is typically in the range of 20-60 Å. The rate of energy transfer from a donor to an acceptor (k_T) is given by

$$k_T = \tau_d^{-1}(R_0 / r)^6 \qquad (8)$$

where τ_d is the decay time of the donor in the absence of acceptor, R_0 is the Forster distance, and r is the donor-to-acceptor distance. When the D-A distance is equal to the Forster distance ($r = R_0$), the transfer efficiency is 50%. At this distance ($r = R_0$), the donor emission would be decreased to one-half of its intensity in the absence of acceptor. The rate of RET depends on strongly on distance, being inversely proportional to r^6. If the transfer rate is much faster then the decay rate, then the energy transfer will be efficient. If the transfer rate is slower than the decay rate, then little transfer will occur during the excited-state lifetime. The efficiency of energy transfer (E) is the fraction of photons absorbed by the donor that are transformed to the acceptor. This fraction is given by:

$$E = k_T / (\tau_D^{-1} + k_T) \qquad (9)$$

This is the ratio of the transfer rate to the total decay rate of the donor. Recalling that $k_T = \tau_D^{-1} (R_0 / r)^6$, one can easily rearrange equation (9) to yield

$$E = R_0^6 / (R_0^6 + r^6) \qquad (10)$$

The transfer efficiency is typically measured using the relative fluorescence intensity of the donor, in the absence (F_D) and presence (F_{DA}) of acceptor. The transfer efficiency can also be calculated from the lifetimes under these respective conditions:

$$E = 1 - \tau_{DA} / \tau_D \qquad (11)$$

$$E = 1 - F_{DA} / F_D \qquad (12)$$

It is important to know the assumption involved in the derivation of these equations. Equations (11) and (12) are only applicable to donor-acceptor pairs which are separated by a fixed distance. For the case where a range of D-A distances is possible, the presence of a distribution of distances has a profound impact on the time-resolved decays of the donor. The range of distances results in a range of decay times, so that donor decay becomes more complex than a single exponential. Similar results are expected for F_D data. The goal of most distance distribution studies is to recover the D-A probability distribution from the nonexponential decays of the donor. It is important to notice the necessity of the time-resolved data. Under these circumstances, the steady-state data can not be used to determine the distance distribution, and they will not even reveal the presence of a distribution. It is not possible to determine a distance

distribution of arbitrary shape. So, it is common practice to describe the distribution using a limited number of parameters.

The donor intensity decay is a summation of the intensity decays for all accessible distances and is usually written as:

$$I_{DA}(t) = \int_{r=0}^{\infty} P(r)\, I_{DA}(r, t)\, dr$$

$$= I_D^0 \int_{r=0}^{\infty} P(r) \exp[-t / \tau_D - t(R_0 / r)^6 / \tau_D]\, dr \qquad (13)$$

Data analysis is performed by predicting the values of I_{DA} (t) for use with T_D or F_D measurements and the usual procedures of nonlinear least squares. Typically, the decay time of the donor (τ_D) is known from measurements of the donor in the absence of acceptor. The variable parameters in the analysis are those describing the distance distribution.

I.3 Experimental Design

I.3.1. Design of Rigid Crown Ether/Ammonium Salt Molecules

The molecule selected for the present series of studies on photoinduced electron transfer reactions appears in Figure 2.

Dimethoxynaphthalene was chosen as the electron donor, and quinone, naphthaquinone as electron acceptor. Different substituents will be incorporated into the acceptor in order to determine the dependence of k on ΔG°.

The para-dimethoxynaphthalene was chosen as the electron donor for the following reasons.

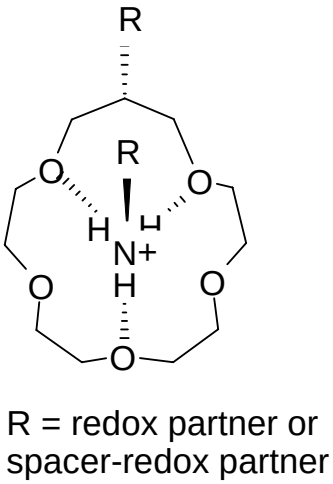

Figure 2. General structure of the target molecule

First, para-dimethoxynaphthalene was used as electron donor by previous other studies on electron transfer reactions; Second, synthetic facility and its stability make it in wide application conditions.

The decision to use benzoquinone and naphthaquinone as the electron acceptor was based primarily on their having the appropriate redox properties and their synthetic versatility. The quinone group allows for the fairly convenient variation of the reaction driving force by changing the substituents on the ring.

Many different types of spacers have been used, but two main categories are modified proteins and peptides [26,27] and saturated hydrocarbon. [28-32] Generally, bicyclooctane spacers have been used in studies of energy transfer between aromatic and carbonyls and electron exchange in aromatic anions, [33,34] as well as intramolecular charge transfer reactions involving amine groups. [35] The principal advantages of using a fully hydrocarbon spacer rather than amides or esters lie in its chemical inertness which permits its application in basic, neutral, mildly acidic, or nucleophilic conditions. Another advantage is its structural rigidity, which enforces a fixed separation distance with an angle of 180° between the donor and acceptor. For example, bicyclo[2.2.2]octane is highly symmetric, thereby simplifying considerations of the presumed through-bond pathway for electron transfer.

The structures of redox partners and spacers are summarized in Figure 4.

Several features of these complexes are noteworthy. First, CPK and computer modeling suggested that the steric bulk of the substituent on the crown ether will highly favor the geometry pictured as shown in Figure 3. Use of the 16-crown-5 ether derivative also favors the ammonium salt coordination geometry (by three oxygens) shown, as was observed in similar complexes.[36,37] These two features should ensure a symmetrical complex with a single shortest through-bond ET route; the bicyclic spacers will help rigidify the complexes.

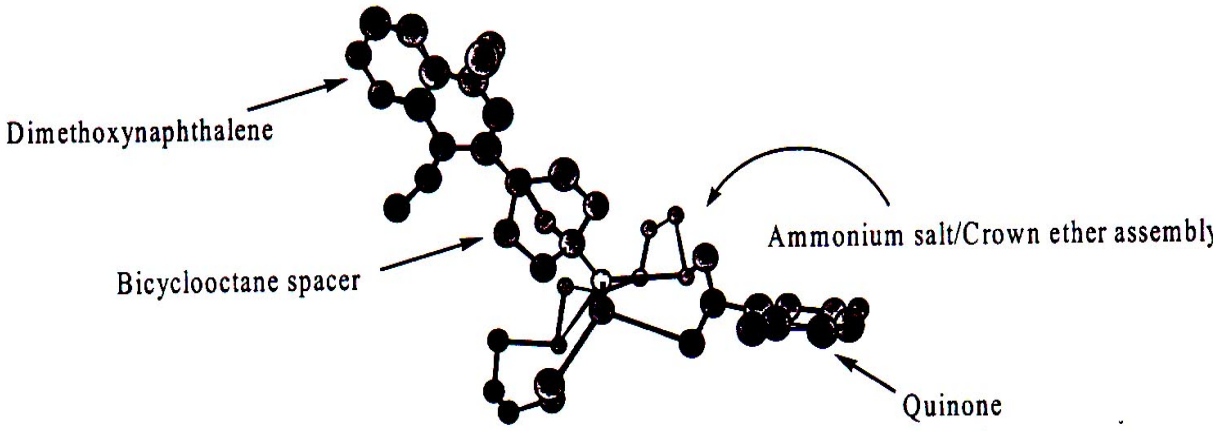

Figure 3. Chem 3-D model of proposed crown ether / ammonium salt complex with a dimethoxynaphthalene donor linked via a bicyclooctane spacer to an ammonium salt and a quinone attached to a crown ether.

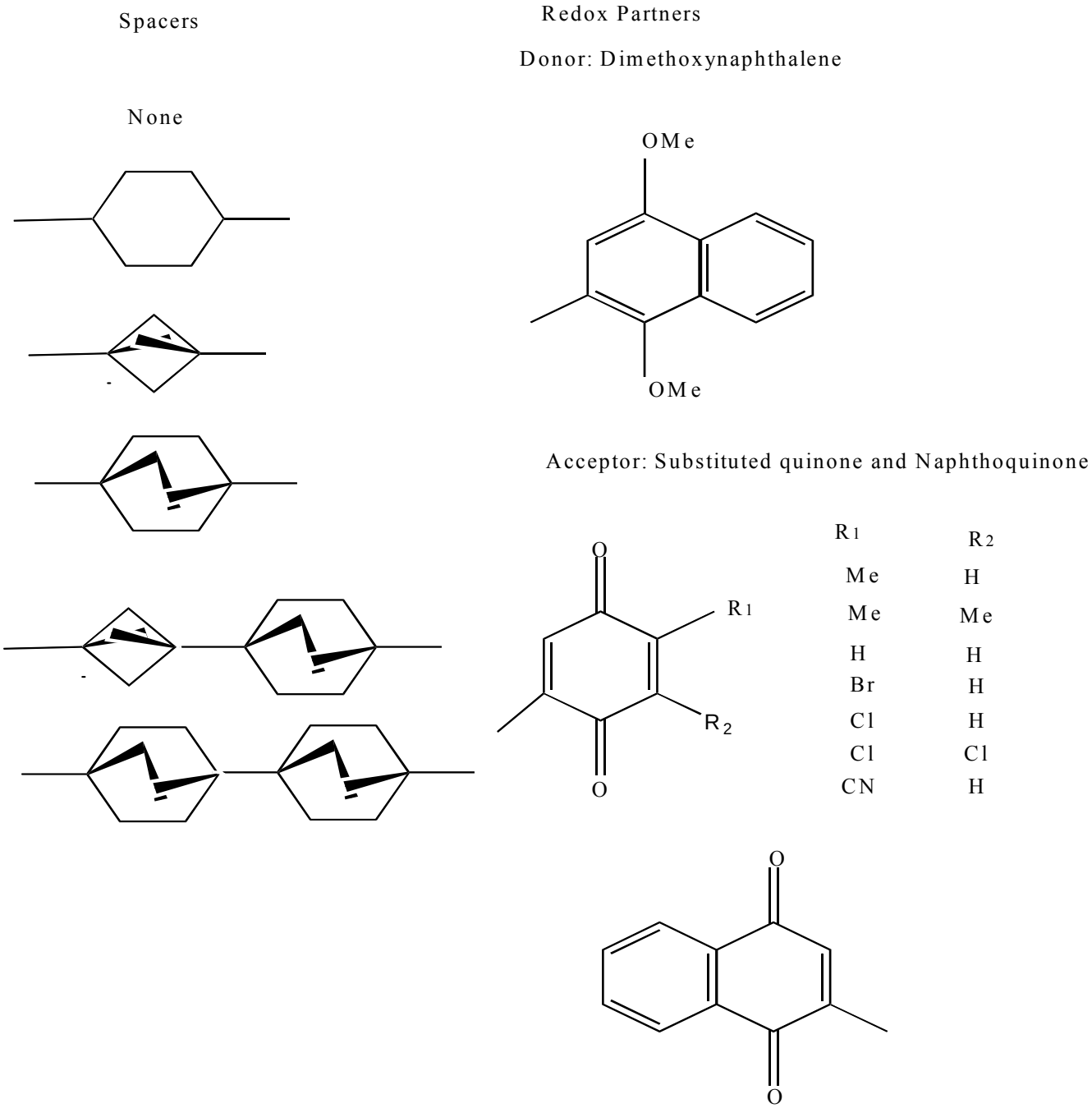

Figure 4. General structure for electron transfer donors, acceptors and spacers.

I.3.2 Synthetic Strategies

With the structural requirement set forth, a need remained for an adequate synthetic route. In the

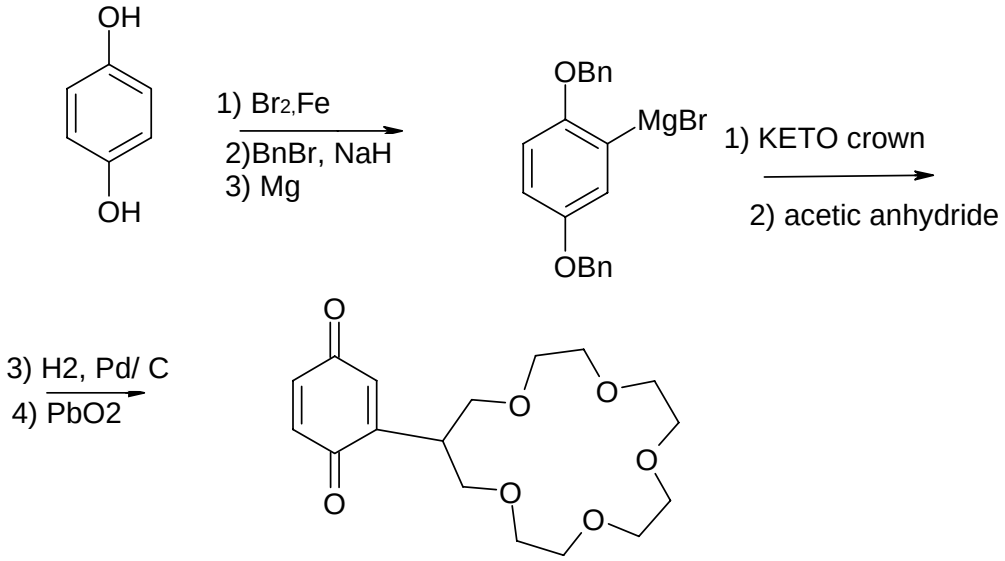

Scheme 1

first research phase, complexes will feature the crown ether directly attached to the dimethoxynaphthalene donor and the ammonium salt to the substituted quinines and naphthaquinones. In the advanced research phase, generation systems will incorporate the rigid bicyclic spacer into the complexes and also put the redox donor on the ammonium salt and acceptor on the crown ether.

The key keto crown ether precursor (where R on crown ether is = O in Figure 1) for the complexes, can be prepared by known chemistry in two steps from commercially available tetraethylene glycol and 3-chloro-2-chloromethyl-1-propene in 35 % overall yield. [38] After we prepare this precursor, we can obtain several target crown ether -(spacer) -donor/acceptor compounds; two examples are shown in Scheme 1 & 2.

Zimmerman *et al.* in 1980 reported their studies on rod-like organic molecules working with bicyclic spacers. [34] For the [1]-rod syntheses, they utilized 1,4-dichlorobicyclo[2.2.2]-octane which was obtained by the method of Kauer as the starting material. [39] This synthesis is outlined in Scheme 3.

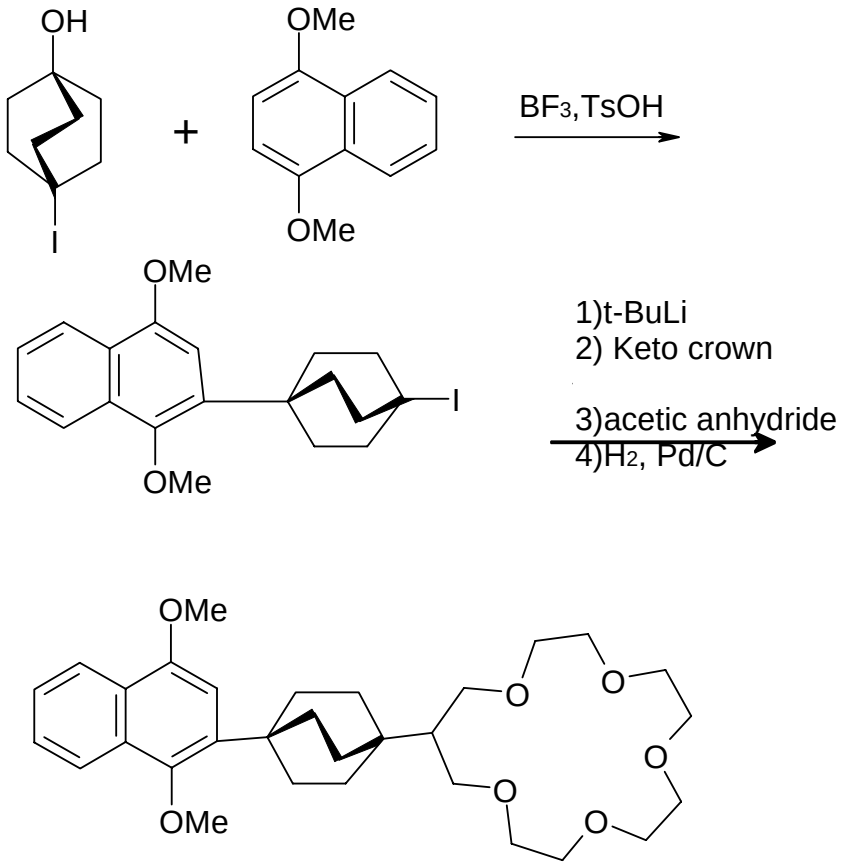

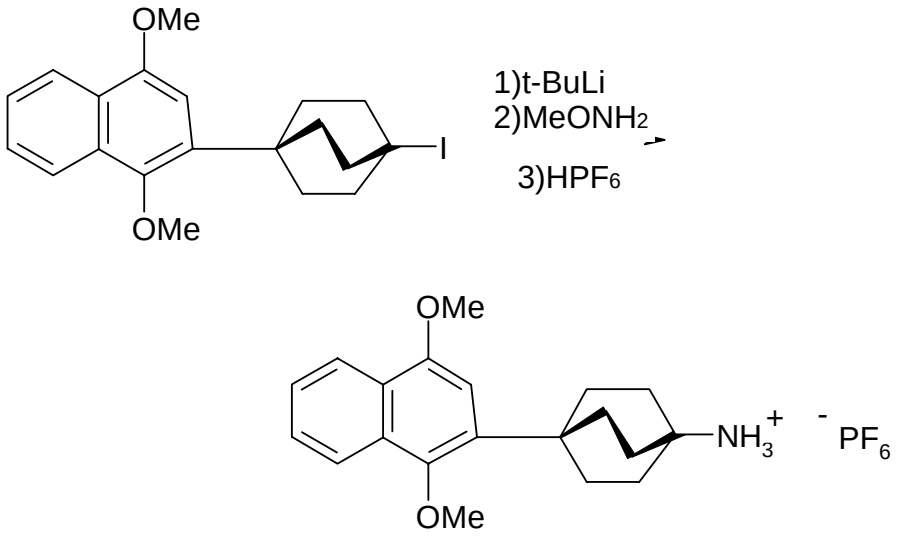

Scheme 2

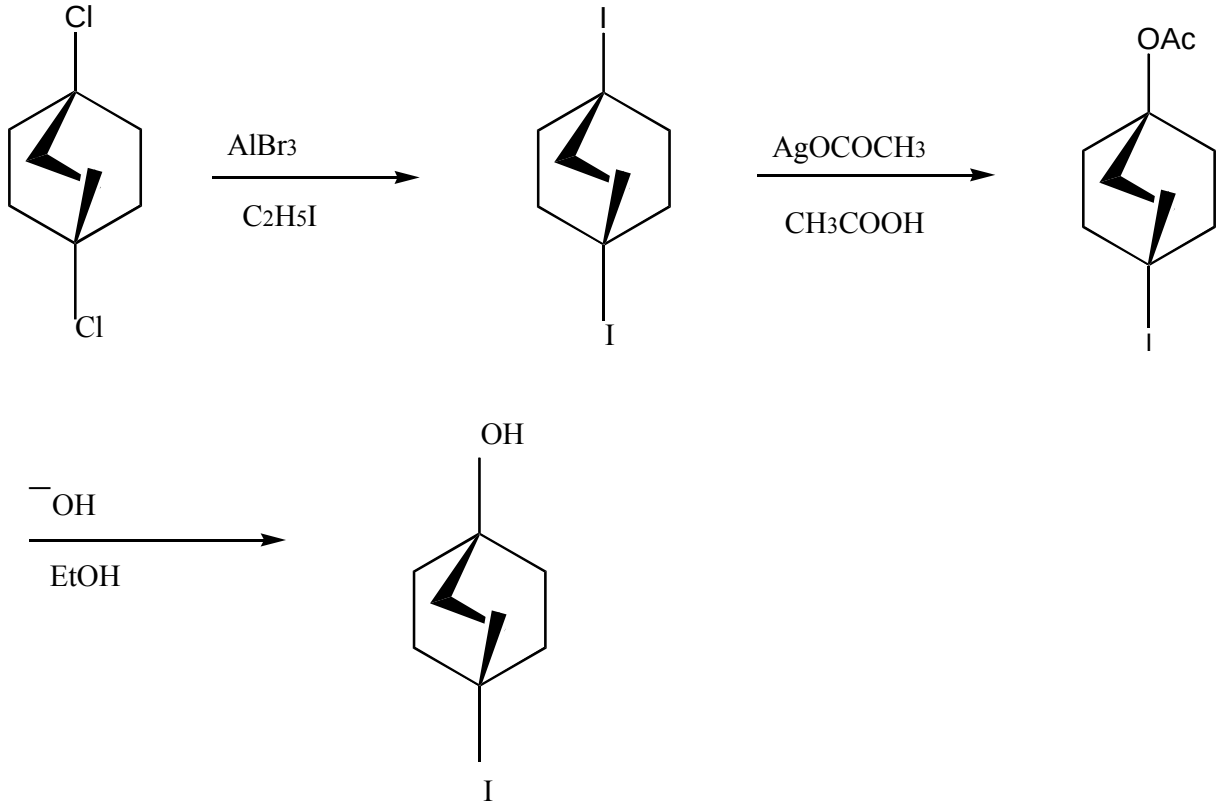

Scheme 3

For the [2]-rod synthesis (Scheme 4), they observed that reaction of 1-iodo-4-methoxybicyclo[2.2.2] octane with magnesium in ether led to ca. 65-70% yields of 4,4'-dimethoxy-1,1'-bibicyclo[2.2.2]-octyl in the presence of either nickelous chloride or silver iodide in molar quantities as catalyst.

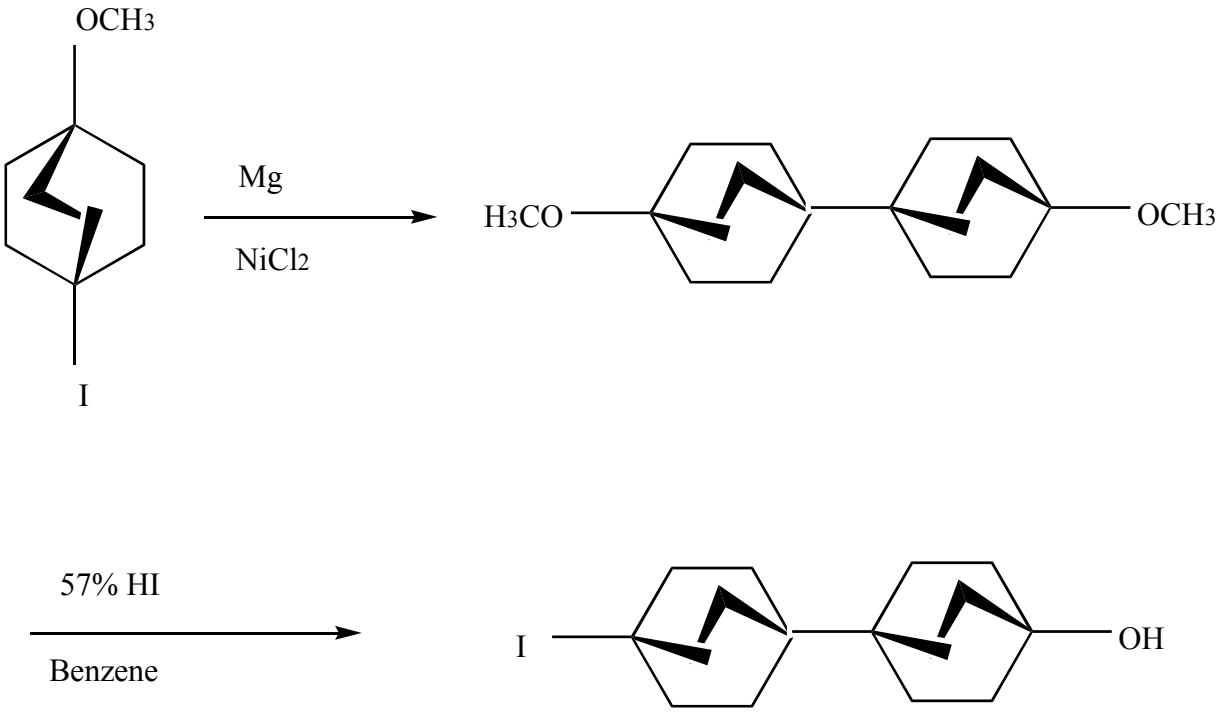

Scheme 4

The quinone ammonium salt can be prepared by routes as that shown in Scheme 5 by the known chemistry except the last step. [40]

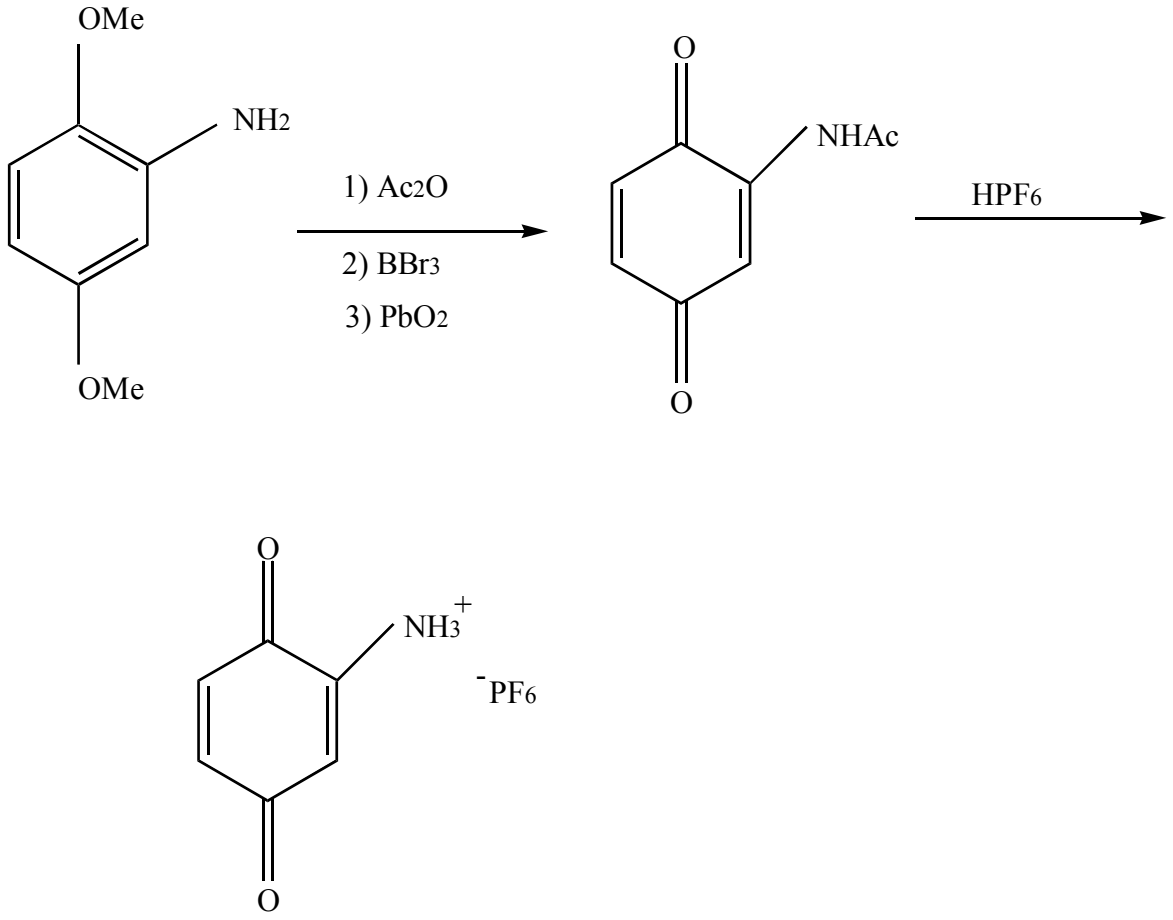

Scheme 5

In this thesis, I chose the target molecules as shown in Figure 5.

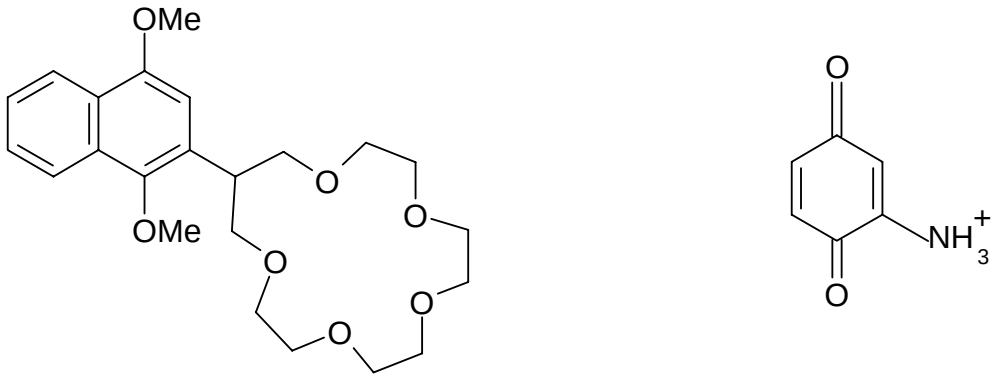

Figure 5. Feature target molecules

II. Results and Discussion

II.1 Synthetic Aspects and Characterization of Electron Donor Part

The procedures employed to prepare the key intermediate for the electron donor molecule and its precursors are shown in Scheme 6.

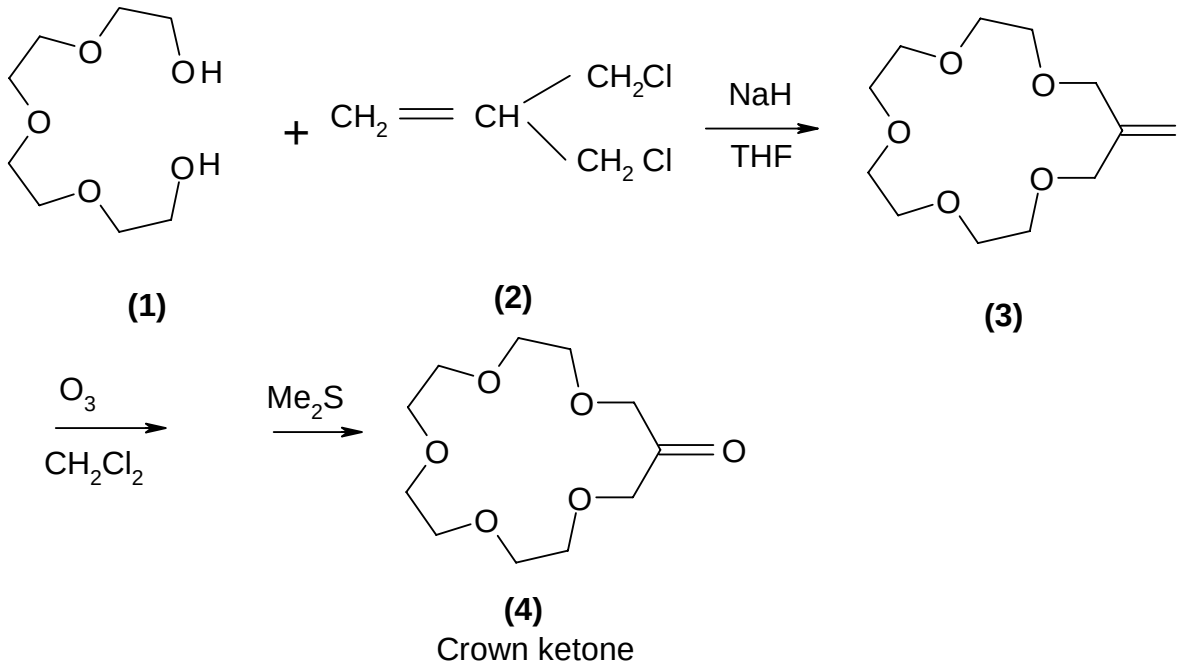

Scheme 6

Tomoi *et al.* in 1978 reported their studies on the syntheses of hydroxy group containing crown ethers. For the crown ethers with vinylidene group, they used 3-chloro-2-chloromethyl-1-propene and appropriate glycols in 35% yield.[38]

Based on our target molecule, commercially available 3-chloro-2-chloromethyl-1-propene **2** and tetraethylene glycol **1** are chosen as the starting materials, and sodium hydride was employed as base. The corresponding methylene crown ether **3** was obtained in about 30% yield. The low yield of this reaction is attributed to the formation of dimer during the process. The ^{1}H NMR spectrum of **3** revealed one singlet at $\delta = 5.17$ for the two methylene protons. The IR spectrum of **3** has a weak absorption at 1650 cm^{-1} for C=C bond.

Henne *et al.* [42] used zinc and water in the presence of acetic acid to decompose of ozonide from crown ether **3**. Lin *et al.* reported in 1996 that ozonolysis in dichloromethane at -78°C followed by reduction with dimethyl sulfide to give

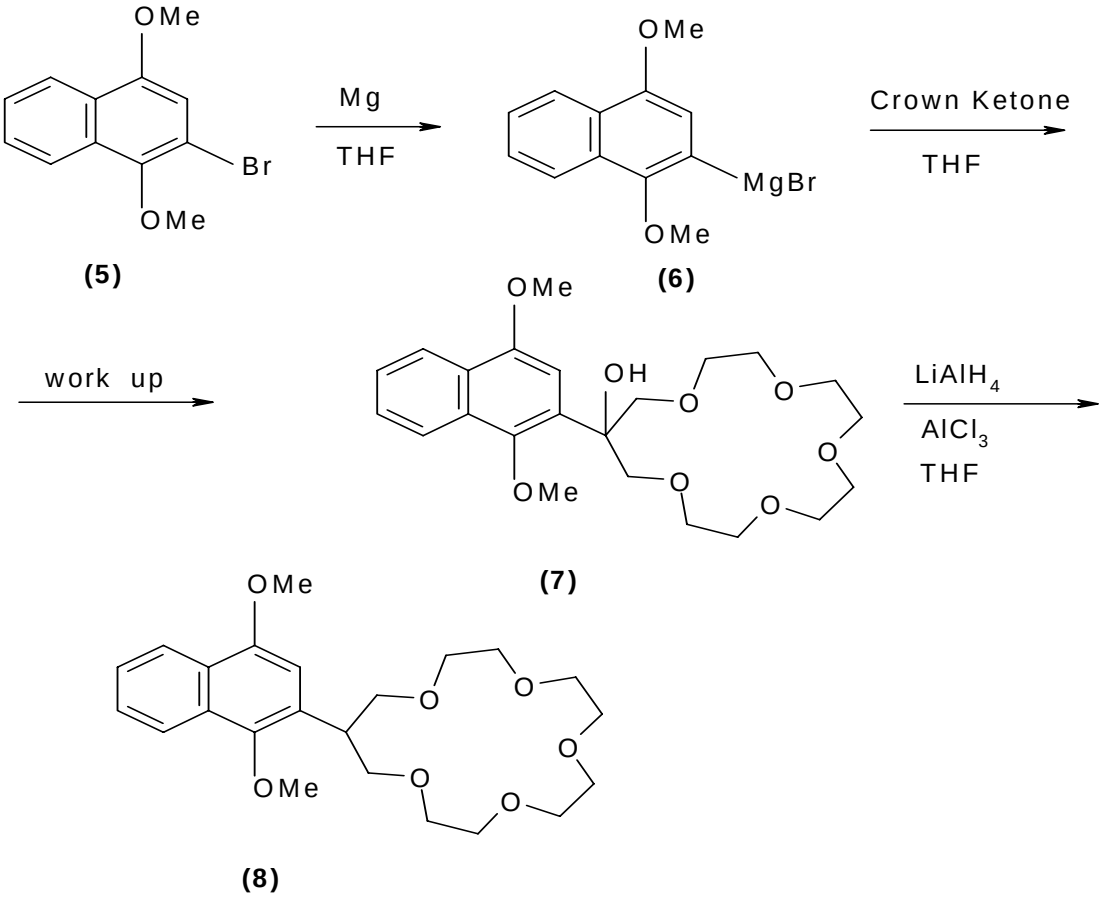

Scheme 7

the corresponding keto crown ether in 80-85 % yield. We followed the latter method to obtain this key intermediate crown ether keto **4**. [43]

The IR spectrum of **4** lacked alkene absorptions and showed a strong absorption near 1735 cm^{-1} for the carbonyl C = O bond. In the ^{1}H NMR, the absorption at $\delta = 4.17$ singlet for the protons adjacent to the methylene group of **3** shifted to $\delta = 4.46$ for the protons now adjacent to the carbonyl group of **4**. The ^{13}C NMR spectrum of **4** displayed one peak at $\delta = 207.46$ for the carbonyl carbon.

The remaining steps to prepare the final target molecules are shown in Scheme 7.

The method employed to prepare crown ether alcohol **7** is the Gringard reaction. Two kinds of catalysts iodine and 1,2 – dibromoethane are utilized in this reaction. The result showed that iodine is better for obtaining a slightly higher yield. We believe this low yield is due to two reasons: (1) steric hindrance of the reactants; and (2) since there are five oxygen atoms in **7**, this molecule has a moderate solubility in water, and therefore, some amount of product was lost during the quenching and extracting processes.

The ^{1}H NMR spectrum of **7** showed that it possesses moieties of dimethoxynaphthalene and 16-crown-5. The absorption at $\delta = 4.99$ singlet demonstrates the existence of hydroxy group on **7**. The IR spectrum of **7** also confirms that information, since there is a weak, broad absorption near 3495 cm^{-1}.

For the final product **8**, at first we designed the synthetic route shown in Scheme 8 based on the known chemistry. The first step is dehydration, and the second is hydrogenation. The intermediate **9** was obtained in moderate yield, 62%, using acetic anhydride and sodium bicarbonate. The last step did not work well, and no product was obtained.

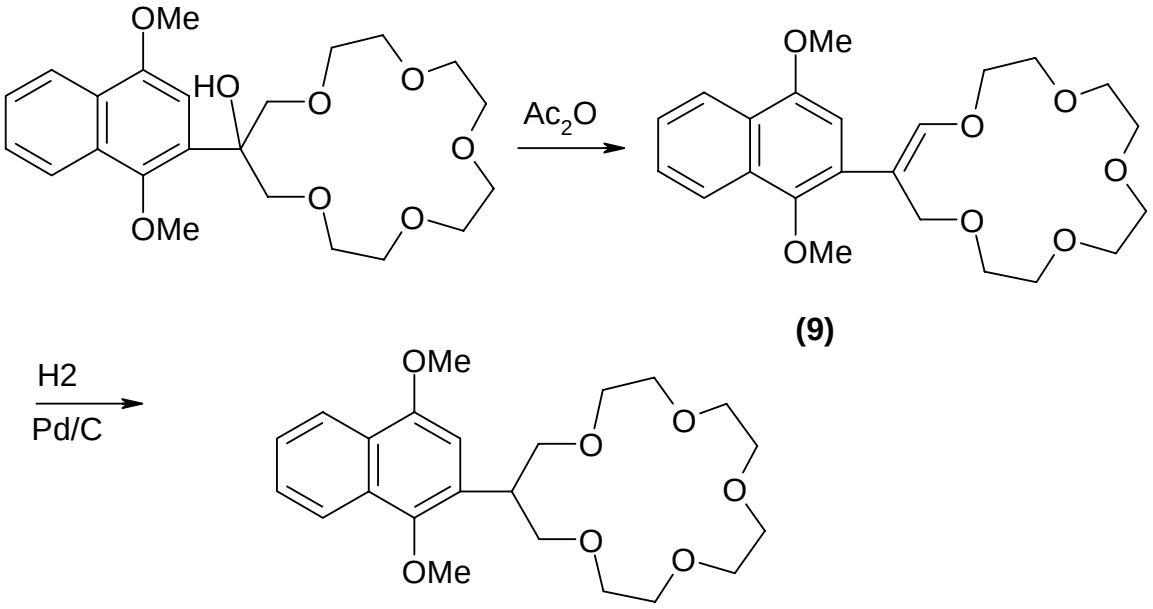

Scheme 8

The ^{1}H NMR spectrum of the product showed signals of the dimethoxynaphthalene moiety, however, the peaks of the crown ether moiety disappeared. We believe the failure resulted from prolonged duration of hydrogenation (about 2 days) at room temperature.

Brester *et al.* reported the reduction of saturated alcohols to hydrocarbons by "dichloroaluminum hydride" at 60-80°C in high-boiling ethers.[41] We followed this procedure as shown in Scheme 6

to obtain the final target compound **8**. In this reaction, aluminum chloride and lithium aluminum hydride were employed as hydrogenolysis agents in THF at reflux temperature to afford the corresponding compound **8** in 60% yield. The main advantage of using this procedure is that the overall yield increases, since only one step is needed to get **8**, compared to two steps needed in Scheme 8 with moderate yield for each step.

The IR spectrum of **8** lacked hydroxy absorptions near 3500 cm^{-1}. In the ^{1}H NMR, the absorption at δ = 7.29 singlet for the proton on the β-carbon position of dimethoxynaphthalene ring of compound **7** shifted to δ = 6.46 for the same position proton of compound **8**. The chemical shift change is due to the removal of the hydroxy group of compound **8**.

II.2 Synthetic Aspects and Characterization of Electron Acceptor Part

The procedures to obtain the electron transfer acceptor part -- ammonium quinone salt are shown in Scheme 9.

The starting material for the electron transfer acceptor portion is 1,4-hydroxyquinone (**10**). The base- promoted reaction of **10** with excess dimethyl sulfate produced the corresponding dimethoxybenzene **11** in 90 % yield by a known procedure.

The method employed to prepare **12** is based on the work of Herbert *et al.* They utilized concentrated nitric acid in acetic acid at 30°C to react with **11** to produce the mononitration compound **12**. We followed this procedure to try to obtain mononitro compound **12**, but failed.

The GC-MS spectrum of the product displayed the molecular ion peak (m/z) at 228, which is identical to the molecular weight of dinitro-1,4- dimethoxybenzene. The strong nitrating nature of concentrated nitric acid is responsible for the formation of this dinitro compound. We modified the above method by diluting concentrated nitric acid with water (volume ratio 1:2) and repeated this reaction at room temperature to give mononitro product **12** in 92% yield. The ATP ^{13}C NMR spectrum of **12** showed three absorptions at $\delta = 110.4$, $\delta = 115.6$ and $\delta = 121.07$ respectively, and one proton is connected to each of these carbons. This spectrum showed

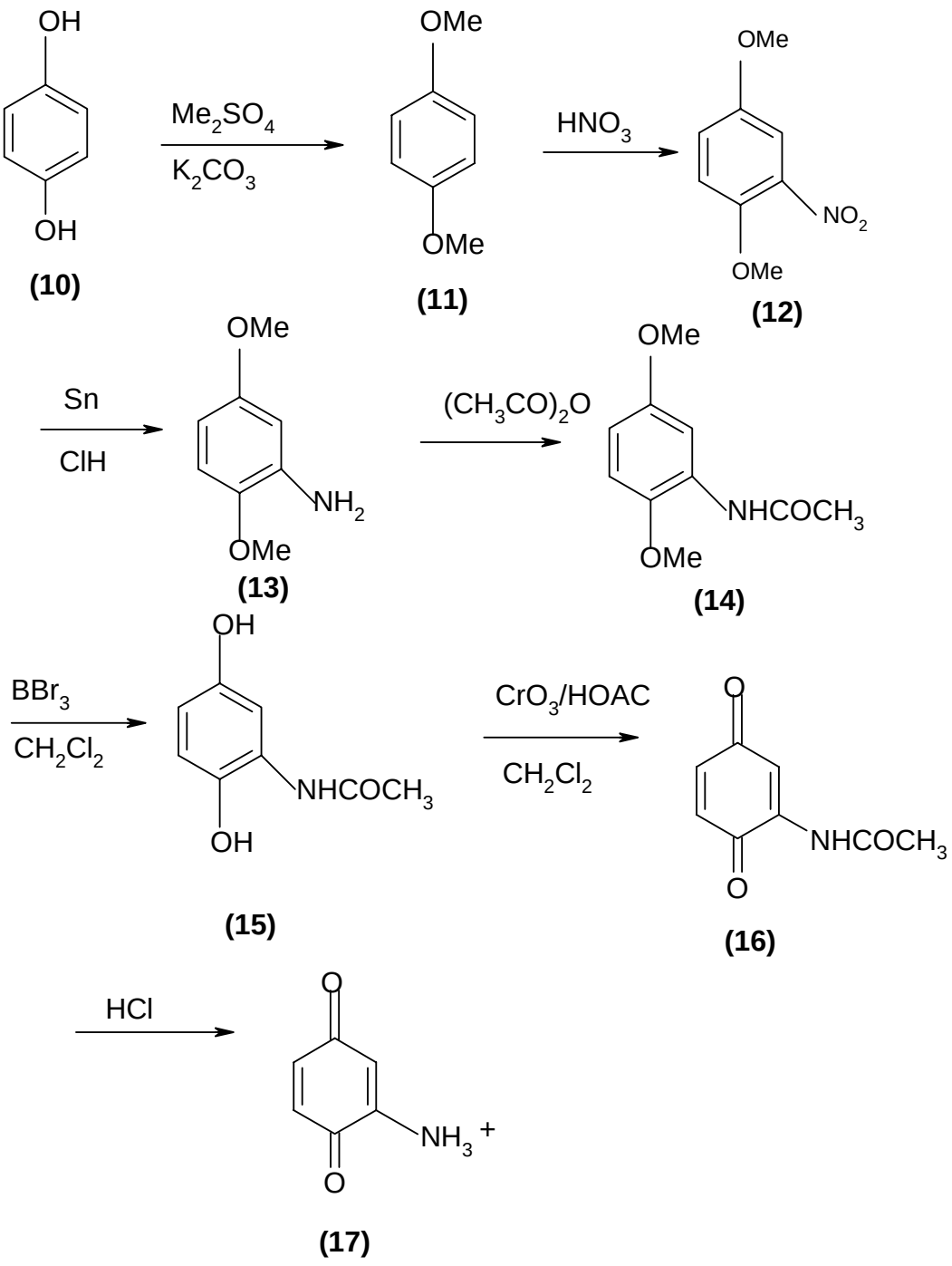
OH
OH
(10)
Me2SO4
K2CO3
OMe
OMe
(11)
HNO3
OMe
NO2
OMe
(12)
Sn
ClH
OMe
NH2
OMe
(13)
(CH3CO)2O
OMe
NHCOCH3
OMe
(14)
BBr3
CH2Cl2
OH
NHCOCH3
OH
(15)
CrO3/HOAC
CH2Cl2
O
NHCOCH3
O
(16)
HCl
O
NH3 +
O
(17)

Scheme 9

three carbon positions on the benzene ring were substituted, and the other three positions still were unsubstituted. The ration of 4 different kinds of protons in the ^{1}H NMR spectrum also confirms the structure; it is 1:2:3:3.

Reduction of nitro aromatic compound **12** followed by acylation of amine **13** was a general procedure in satisfactory yields. The ^{1}H NMR spectrum of **13** showed aromatic protons were downfield shifted by 0.6 ppm to 6.68-6.71 and 6.21-6.32 with respect to those in the precursor **12**. This is due to the conjugate effect of amino group. Acetic anhydride was used as an acylating agent and solvent for the step converting **13** to **14**. The ^{1}H NMR of **14** showed the protons on the benzene ring shifted downfield with respect to the aromatic protons of **13**. The carbonyl group exerts an induction effect and conjugates with the -NH group, which is responsible for this deshielding. The singlet at $\delta = 2.20$ showed methyl protons on the acetyl group.

Compound **15** was obtained in moderate yield by utilizing boron tribromide in dichloromethane at -78°C. The ^{1}H NMR spectrum of **15** showed that two proton singlets on the methoxy groups disappeared with respect to those of **14**. The chemical shifts for the other protons, including aromatic and methyl protons on the acetyl group, do not change very much. This is mainly due to the small effect of methoxy group exerting on these protons.

Acid promoted oxidation of **15** by chromium trioxide in glacial acetic acid produced quinone **16**. This reaction went very well, even though chromium trioxide in acetic acid is a very strong oxidizing agent, since no groups attached to benzene ring are sensitive to the oxidizing medium. The ^{1}H NMR spectrum showed a multiplet at $\delta = 6.75$-6.82, characteristic of absorption of

quinone protons. The methyl protons on acetyl group were a singlet which shifted 0.2 ppm downfield with respect to the methyl protons in precursor **15**.

For our final target molecule, an ammonium quinone salt, we employed several methods to try to synthesize it; however, all methods failed.

Diluted hydrochloric acid was used to hydrolyze the amide group at reflux under an argon atmosphere to obtain salt **17**. After reaction, the solvents were evaporated in vacuo, and the solid was collected. In the ^{1}H NMR of this solid, only some absorptions at δ = 1.3-1.5 ppm and δ = 3.8-3.9 ppm were observed. No absorptions around δ = 6.8-7.0 ppm were observed. We think that the reduction nature of

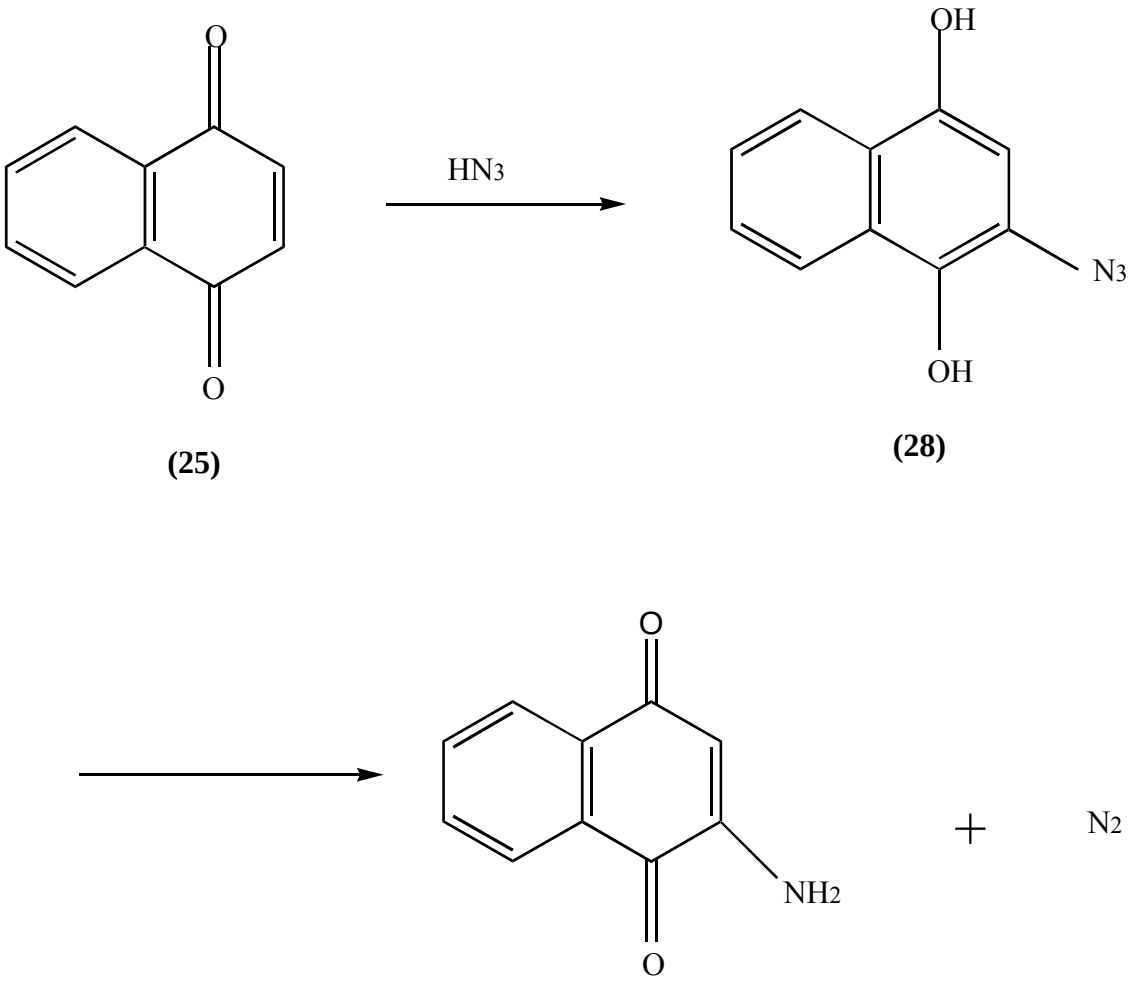

(25) **(28)** **(26)**

Scheme 10

chloride and the strong acidity of hydrochloric acid are responsible for this failure. We followed the same procedure except replacing hydrochloric acid by hexaflurophosphoric acid; however, still no compound **17** was obtained in this way.

Cason pointed out that relatively few aminoquinones have been prepared, and most of these have been obtained only as acetyl derivatives.[45] The amino group is susceptible to both oxidation and

hydrolysis if aqueous oxidizing agents were used. Even for those aminoquinone synthesized successfully, the yields were very low.

Fieser and Hartwell reported their studies on the reaction of hydrazoic acid with naphthoquinones.[46] They proposed a very convenient means of obtaining the amino derivatives of naphthoquinones in high yields by utilizing sodium azide and 1,4-naphthoquinone in glacial acetic acid at 40°C. They also proposed a mechanism for this reaction (Scheme 10). They also mentioned the reactivity difference between benzoquinone and naphthoquinone for this reaction. With benzohydroquinone, azidobenzohydroquinone (see Scheme 10) is sufficiently stable to be isolated because the reducing group of the molecule is not sufficiently potent to interact with the reducible azido group; on the other hand, with the compound of naphthoquinone series the potential is at a more effective level and interaction occurs.

In other word, we can assume that the oxidizing power of the azido group is approximately the same in each case, but it is certain that naphthohydroquinone would be a more potent reducing agent than benzohydroquinone.

The above theories help to explain why our synthesis of ammonium quinone salt was unsuccessful. The amino group is very sensitive to oxidation, and hydroquinone's oxido-reduction potential is not low enough to make amino quinone stable.

Based on the above result and theories, we redesigned two target molecules as our acceptor portion for our electron transfer study. The first one is 2-amino-1,4-naphthoquinone

hydrochloride. For the second one, we added a bridge, methylene group, between the quinone ring and amino group. We believe this bridge portion can stabilize this molecular structure, since the amino group is not attached to the quinone ring directly, no conjugate effect can occur to make this molecule unstable.

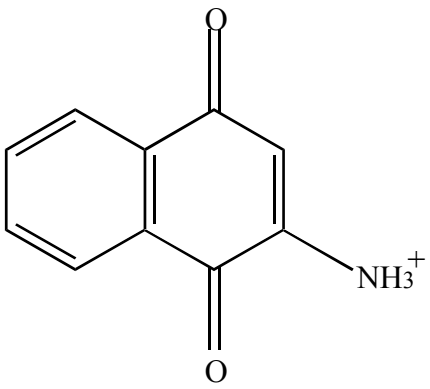

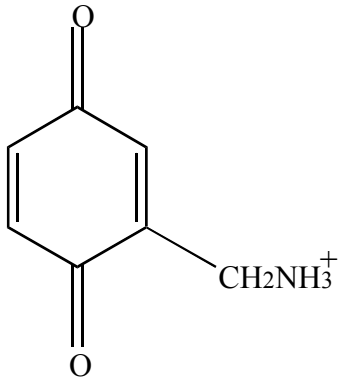

The procedures employed to produce 2-amino-1,4-naphthalene hydrochloride are shown in Scheme 11.

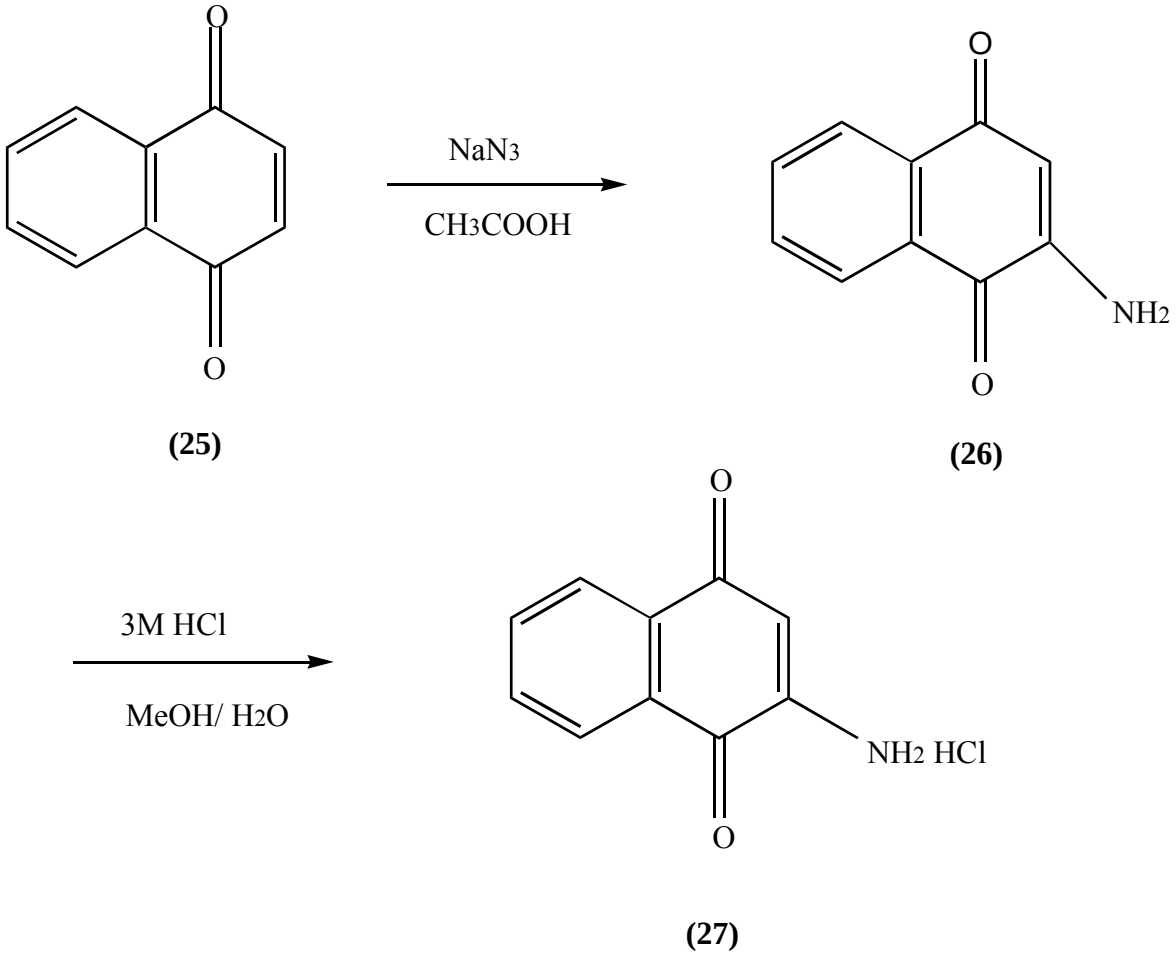

Scheme 11

The amination method in this scheme was based on Fiesher's work. We utilized sodium azide and 1,4-naphthoquinone in acetic acid at 40°C to obtain **26**. The GC-MS spectrum **26** revealed the molecular ion peak at 173 which is identical to the molecular weight of **26**. The ^{1}H NMR spectrum of **26** showed one singlet at δ = 6.00 for the proton on β-carbon of naphthaquinone with respect to one singlet δ = 6.99 for the same position proton of naphthoquinone **25**. The conjugate effect of the amino group is responsible for this shielding.

27 was produced by reacting **26** with 3M hydrochloric acid in methanol at reflux under an argon atmosphere for five hours. The yield is around 80%. The brown yellow solid was precipitated after reaction. The GC-MS of **27** displayed a molecular ion peak at 174 which is identical to the molecular weight of the naphthoquinone ammonium cation portion. The absorption at $\delta = 6.19$ for the proton on β-carbon of **26** shifted to $\delta = 6.19$ for the proton on β-carbon of **27**. This deshielding is due to the inductive effect of NH_3^+ and loss of the conjugating system of **26**.

The methods used to produce benzyl quinone ammonium salt are shown in Scheme 12.

The general method of Riche, Gross and Hoft was employed to obtain aldehyde **18**. In this reaction, α,α-dichloromethyl methyl ether and stannic chloride were stirred at 0°C to give the desired product **18** in 65 % yield. The proton on the aldehyde was a singlet at $\delta = 10.44$ ppm. Hydroxylamine hydrochloride, and sodium formate in 95% formic acid were employed to react with **18** at reflux for six hours to obtain cyano substituted dimethoxybenzene **19**. In the ^{1}H NMR spectrum of **19**, the signal at $\delta = 10.44$ ppm disappeared compared to its precursor **18**. The chemical shift of aromatic protons was upfield 0.2 ppm with respect to aromatic protons on **18** due to the lower inductive effect of the cyano group. The GC-MS spectrum also confirmed this structure by showing a molecular ion peak at 163.

Cyano reductions with lithium aluminum hydride were not very high yielding. In the case of **19**, lithium aluminum hydride was stirred in a molar ratio 1:4 at room temperature overnight to give **20** in 67% yield. The ^{1}H NMR spectrum of **20** revealed one singlet at $\delta = 2.15$ for two protons on

the methylene group which is attached to the benzene ring directly. The aromatic protons got upfield shifted by 0.2 ppm with respect to those in the starting material **19**.

Instead of using acetic anhydride as an acetylating agent, acetyl chloride and triethylamine were employed to produce **21** in 75 % yield. The main advantages of using acetyl chloride are higher yield, shorter reaction time and easier purification and separation. In the ^{1}H NMR spectrum of **21**, one singlet at δ = 1.99 for three protons on the methyl of acetyl group –$NHCOCH_3$, and one doublet at δ = 4.37 – 4.40 resulted from the absorption of methylene protons on the carbon connected to the benzene ring directly. The molecular ion peak m/z = 209 appears in the GC-MS spectrum of **21**.

Demethylation of **21** was utilized using the same method as demethylation of **14** using boron tribromide in dichloromethane at -78°C. The yield of this reaction was not as high as expected. This can be attributed to the high activity of benzyl protons; that proton can be substituted by bromide. The ^{1}H NMR spectrum of **22** showed that two singlets for protons on the methoxy groups disappeared with respect to those of **21**. One doublet at δ = 4.21-4.24 resulted from absorption of benzal protons. The aromatic protons showed absorptions as multiplet at δ = 6.63-6.93. The chemical shift of methyl protons of acetyl group -$NHCOCH_3$ does not change too much at δ= 1.96 with respect to **21**.

Lansinger et.al. reported their demethylation with boron triiodide in 1979. [47] They utilized boron triiodide in dichloromethane to react with p-dimethoxybenzaldehyde at 0°C to obtain p-dihydroxybenzaldehyde in 47% yield. This reaction just needs one to two minutes to finish.

Another advantage to use triiodide is that increased nucleophilicity of boron triiodide affords ether cleavage selectively and less benzal bromide was formed in the system. This method is still under investigation in our lab for demethylation of **21**.

For compound **23**, we followed the same procedure as for compound **15**. Chromium trioxide in acetic acid was employed to convert hydroquinone **22** to quinone **23**. 3M hydrochloric acid was used to hydrolyze the amide group to form amino group and then form the ammonium salt **24** in

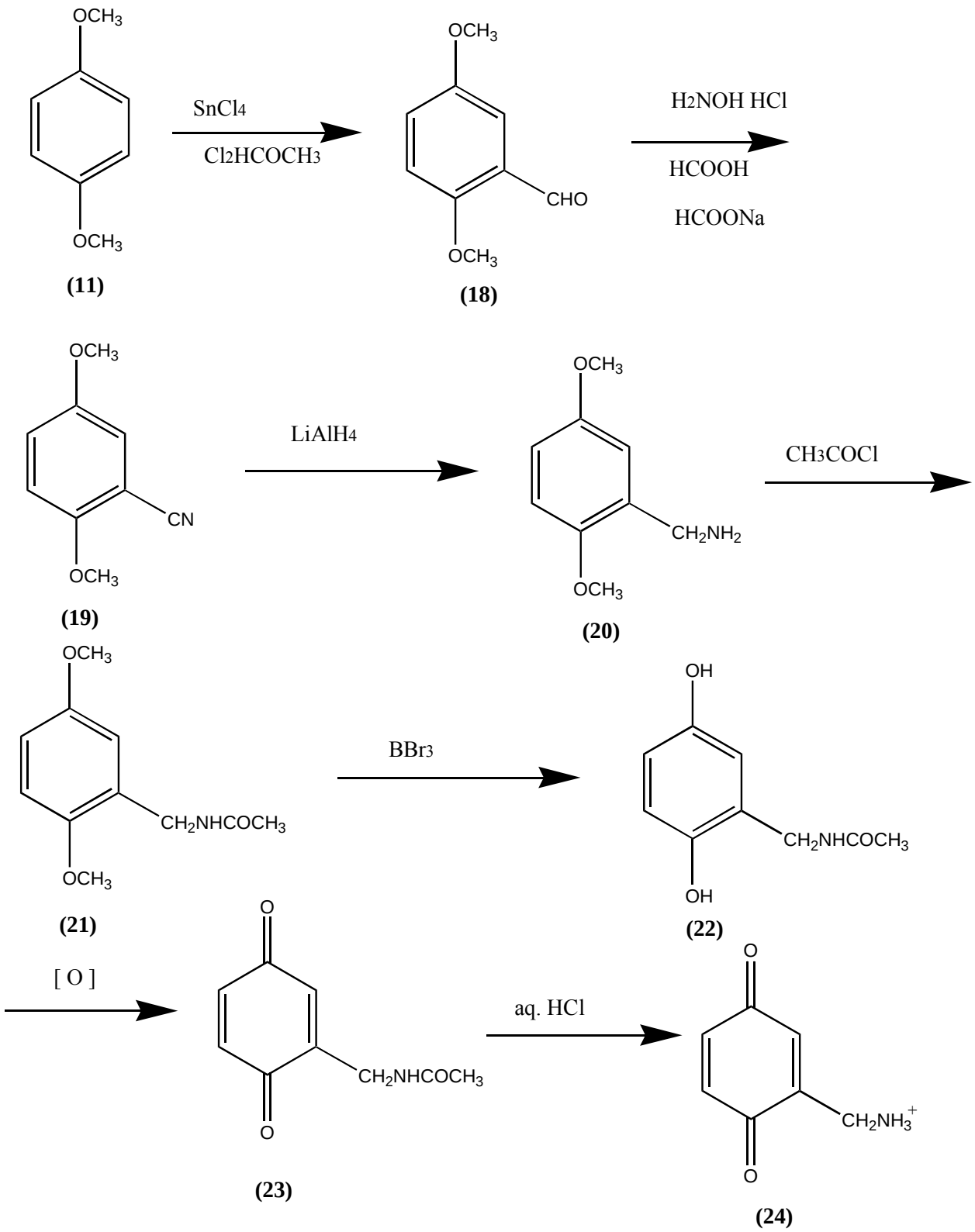
OCH3
OCH3
(11)
SnCl4
Cl2HCOCH3
OCH3
CHO
OCH3
(18)
H2NOH HCl
HCOOH
HCOONa
OCH3
CN
OCH3
(19)
LiAlH4
OCH3
CH2NH2
OCH3
(20)
CH3COCl
OCH3
CH2NHCOCH3
OCH3
(21)
BBr3
OH
CH2NHCOCH3
OH
(22)
[O]
O
CH2NHCOCH3
O
(23)
aq. HCl
O
CH2NH3+
O
(24)

Scheme 12

one pot. The identification of compound **23** and **24** by ^{1}H NMR and GC-MS has not been completed.

II. 3. Complexes Characterization:

The complexes can be characterized based upon well-known analytical techniques, such as UV/vis, NMR, and X-ray crystallography.[48,49] The association constant (K_a) defined in eq (13) has been determined at 24°C in chloroform in which H is the host, G^+X^- is the guest salt, and G^+HX^- is the complex. The guest includes a series of metal picrates and also the dimethoxybenzene ammonium precursor of one of our quinone targets. The host is our initial crown ether compound 16-crown-5 methylene **3**.

$$H + G^+X^- \leftrightarrow G^+HX^- \quad (13)$$

By UV/vis titration method, solution of crown ether 3 in chloroform was used to extract water solutions of sodium, potassium, cesium, rubidium, and ammonium picrates. From the measurement of the ultraviolet (UV) absorbance of the organic phase at 380 nm, the molar ratios of picrate to host (R) were determined at 24°C. With eq. (14), [50] K_a values defined in eq. (13) were calculated. In eq. (14) , K_d is the distribution constant (see eq. 15) of the picrate salts between the two layers in the absence of host, $[G_i]_{H2O}$ is the initial concentration of the picrate salt in water, $[H_i]_{CHCl3}$ is the initial host concentration in chloroform, V_{CHCl3} is the volume of chloroform, and V_{H2O} is the volume of water. Table 1 reports the values of K_a obtained.

$$K_a = R / \{(1- R) K_d\{[G_i]_{H2O} - R[H_i]_{CHCl3}(V_{CHCl3} / V_{H2O})\}^2\} \quad (14)$$

$$K_d = [G^+X^-]_{CHCl3} / ([G^+]_{H2O} * [X.]_{H2O}) \quad (15)$$

The values of K_a for the 5 picrate salts and the host **3** vary from a low about 10^4 for Cs^+ to a high of over 10^5 for Na^+. The K_a values for the different guest cations decrease in the following order:

Table 1. K_a Values of complexes in chloroform at 24°C

Guest cation	$R * 10^3$	$K_a * 10^{-3}$ (M^{-1})
Na^+	138.8	819 ± 31
K^+	38.9	85.5 ± 7.4
Rb^+	21.93	23.52 ± 0.06
Cs^+	43.0	19.27 ± 2.05
NH_3^+	0.90	25.14 ± 1.56

Note: R is the molar ratio of picrate to host molecule

$Na^+ > K^+ > Rb^+ \sim NH_3^+ > Cs^+$

These binding constants are in agreement with those determined for related crown ether and guest.[48,50]

III. Experimental

Melting points were determined in capillary tubes with a laboratory melting point apparatus and are uncorrected. Infrared spectra were taken in $CHCl_3$ solution or on neat thin films between NaBr disks on a Nicolet 520 spectrometer.

The ^{1}H NMR spectra were recorded on a Varian Gemini 200 MHz Fourier transform spectrometer and were referenced to chloroform (δ = 7.24); tetramethylsilane (δ = 0.00); and acetone (δ = 2.04). ^{13} C NMR spectra were recorded on a Varian Gemini 200 MHz Fourier transform spectrometer with a center line of internal $CDCl_3$ (δ = 77.0) as reference. All UV measurements were made on a Beckman DU spectrometer at 380 nm at 24°-26°C. All volume transfer was done by syringe. GC-MS spectra were recorded on a HP5870A spectrometer.

The THF and hexanes were dried by refluxing and distillation over potassium/sodium and benzophenone prior to use.

All chemicals needed for the syntheses except mentioned were purchased from Aldrich Company. All column chromatograph was done with silica gel 60 (230-400 mesh ASTM) purchased from EM Science. Glass-backed preparatory TLC plates (500 μm, indicator F254) were provided by Scientific Absorbents Inc.

1,4-Dimethoxybenzene (11)

A 250 ml round bottom flask surmounted by a condenser was charged with hydroquinone (10,5.5 g, 50 mmol), potassium hydroxide (6.72 g, 120 mmol), methanol (50 ml) and water (50 ml). Dimethyl sulfate (9.5 ml, 100 mmol) was added over twenty minutes, and the mixture was heated at reflux for five hours. On cooling, the mixture was poured onto water and dimethyl ether, and organic layer was washed with saturated aqueous sodium chloride, dried over magnesium sulfate, filtrated, concentrated, and purified by flash column chromatograph (ether/n-hexanes = 1:1) to give 6.24 g (yield 90%) of a white crystal 1,4-dimethoxybenzene (11).

^{1}H NMR ($CDCl_3$, δppm): 3.37 (s, 3H), 6.85 (s, 2H)

GC-MS: *m/z* (%) = 138 (M^+), 123, 95, 41

3-Nitro-1,4-dimethoxybenzene (12)

1,4-dimethoxyhydroquinone (**11**, 0.5 g, 3.6 mmol) was dissolved in acetic acid (2 ml) and diluted nitric acid (2 ml concentrated nitric acid / 4 ml water) was added drop wise. The mixture was shaken for five to ten seconds, then poured onto crushed ice. The mixture was extracted with dichloromethane, the organic layer was washed with saturated sodium bicarbonate, water, dried over magnesium sulfate, filtrated, and concentrated to give 0.606g (yield 92%) of a golden yellow crystal 3-nitro-1,4-dimethoxybenzene (**12**).

^{1}H NMR ($CDCl_3$, δppm): 7.03-7.37 (m, 3H), 3.79 (s, 3H), 3.89 (s, 3H)

^{13}C NMR ($CDCl_3$, δppm): 153.8, 147.9, 121.08, 115.63, 110.4, 57.49, 56.40

melting point: 71-72°C (lit. 72-73°C)

2-amino-1,4-dimethoxybenzene (13)

3-Nitro-1,4-dimethoxybenzene (**12**, 1.0 g, 5.46 mmol), tin (2.6 g, 22 mmol) and ethanol (30 ml) were added in a flask. Concentrated hydrochloric acid (5 ml) was added to the flask in small portions. The mixture was heated at reflux until the solution is colorless. The mixture was poured onto ice. Saturated sodium hydroxide solution containing a small amount of sodium hydrosulfite was added to neutralize. The mixture was extracted with dimethyl ether. The organic layer was dried over magnesium sulfate, filtered, and concentrated to give 0.71 g (yield 85%) of a white crystal 2-amino-1,4-dimethoxybenzene (**13**).

^{1}H NMR ($CDCl_3$, δppm): 6.66-6.83 (m, 1H), 6.21-6.32(m, 2H), 3.79 (s, 3H), 3.72 (s, 3H)

2-acetamino-1,4-dimethoxybenzene (14)

2-amino-1,4-dimethoxybenzene (**13**, 1.0 g, 6.53 mmol) was stirred in acetic anhydride (10 ml) for five hours at room temperature followed by hydrolysis on ice. The mixture was neutralized by sodium bicarbonate, extracted with dimethyl ether, dried over magnesium sulfate, filtered, concentrated to give 0.955 g (yield 75%) of a light brown crystal 2-acetamino-1,4-dimethoxybenzene (**14**).

^{1}H NMR ($CDCl_3$, δppm): 8.08-8.09 (d, 1H), 7.71 (br, 2H), 6.21-6.83 (m, 2H), 3.83 (s, 3H), 3.76 (s, 3H), 2.20 (s, 3H)

2-acetamino-1,4-dihydroxybenzene (15)

2-acetamino-1,4-dimethoxybenzene (**14**, 0.165 g, 0.846 mmol) was dissolved in dichloromethane (50 ml). 1.0 M boron tribromide in dichloromethane (2.6 ml, 2.54 mmol) was added at -80°C under argon atmosphere. After one hour, the stirred mixture was warmed to room temperature and stirred overnight. The reaction was quenched with water, extracted with dimethyl ether. The organic layer was dried over magnesium sulfate, filtrated, concentrated to give 0.07 g (yield 50%) of a yellow oil 2-acetamino-1,4-dihydroxybenzene (**15**).

^{1}H NMR (acetone-d^6, δppm): 6.92-7.05 (d, 1H), 6.45-6.69 (m, 2H), 2.17 (s, 3H)

2-acetamino-1,4-benzoquinone (16)

2-acetamino-1,4-dihydroxybenzene (**15**, 0.073 g, 0.437 mmol) was stirred in 60 % acetic acid (1.5 ml) in a flask at 0°C. Chromium trioxide (0.055 g, 0.549 mmol) was dissolved in water (2 ml) and glacial acetic acid (0.4 ml). The chromium trioxide solution was added to the flask drop wise to keep the temperature at 0°C. After that, the mixture was warmed to room temperature. After two hours, the mixture was neutralized by sodium bicarbonate, extracted with dimethyl ether. The organic layer was dried over magnesium sulfate, filtrated, concentrated to give 0.047 g (yield 65%) of a bright yellow crystal 2-acetamino-1,4-benzoquinone (**16**).

^{1}H NMR (aceton-d^{6}, δppm): 8.08-8.09 (d, 1H), 7.82 (br, 1H), 6.57 -6.83 (m, 2H), 2.20 (s, 3H)

1,4-dimethoxybenzaldehyde (18)

The general method of Rieche, Gross, and Hoft was applied in this preparation. Stannic chloride (1,75 ml, 15 mmol) was added to a solution of 1,4-dimethoxybenzene (**11**, 1.022 g, 7.4 mmol) in dichloromethane (25 ml) at 0°C under argon atmosphere. α,α - dichloromethyl methyl ether was added drop wise at 0°C. The stirred mixture was warmed to 25°C over thirty minutes and then heated to 35°C for twenty minutes. The cooled mixture was poured onto ice water, and extracted with dichloromethane. The organic layer was concentrated to provide 0.80 g (yield 65%) of a pure white crystal 1,4-dimethoxybenzaldehyde (**18**). Colorless prisms resulted from recrystallization from dimethyl ether/n-hexane (1:1).

^{1}H NMR ($CDCl_3$, δppm): 10.44(s, 1H), 6.92-7.33 (m, 3H), 3.89 (s, 3H), 3.80 (s, 3H)

2-Cyano-1,4-dimethoxybenzene (19)

In a 50 ml round-bottom flask a solution of 1,4-dimethoxybenzaldehyde (**18**, 0.7 g, 4.22 mmol), hydroxylamine hydrochloride (0.46 g, 6.52 mmol), and sodium formate (0.35 g, 5.12 mmol), in 95% formic acid (20 ml) was heated at reflux for six hours. On cooling, the solution was poured onto ice water, neutralized by sodium bicarbonate, and extracted with dimethyl ether. The

organic layer was washed with saturated aqueous sodium chloride and water, dried over magnesium sulfate, and solvents were evaporated in vacuo to give 0.507 g (yield 74%) of a gray crystal 2-cyano-1,4-dimethoxybenzene (**19**).

^{1}H NMR ($CDCl_3$, δppm): 6.87-7.11 (m, 3H), 3.88 (s, 3H), 3.78 (s, 3H)

GC-MS: *m/z* (%) = 163 (M^+), 148, 120, 79, 65, 62, 51

2,5-dimethoxybenzylamine (20)

A solution of 2-cyano-1,4-dimethoxybenzene(**19**, 0.23 g, 1.41 mmol) in anhydrous dimethyl ether (10 ml) was added during 10 minutes to a stirred 1M solution of lithium aluminum hydride in anhydrous dimethyl ether (16 ml). The mixture was kept at 0°C for forty-five minutes and then at room temperature for fourteen hours. At this time, the reaction was quenched by slow addition of water (0.4 ml) and ethyl acetate (16 ml). The mixture was stirred for fifteen minutes, filtered through a plug of Celite, eluted with ethyl acetate (5 ml) and concentrated to yield 0.158 g (yield 67%) of a yellow oil 2,5-dimethoxybenzalamine (**20**).

^{1}H NMR ($CDCl_3$, δppm): 6.73-6.81 (m, 3H), 3.78 (s, 3H), 3.75 (s, 3H), 2.15 (s, 2H), 1.96 (br, 2H)

GC-MS: *m/z* (%) = 167 (M^+), 151, 136, 123, 109, 77, 65.

2,5-Dimethoxybenzalacetanilide (21)

2,5-Dimethoxybenzalamine (**20**, 0.167 g, 1mmol) was dissolved in dichloromethane (5 ml) and triethylamine (0.122 g, 1.2 mmol), and acetyl chloride (0.095 g, 1.2 mmol) was added at 0°C. After stirring at room temperature for one hour, the mixture was diluted with dichloromethane (20 ml) and extracted with water. The organic layer was dried over magnesium sulfate and concentrated in vacuo to give 0.157 g (yield 75%) of a slight yellow oil 2,5-dimethoxybenzalacetanilide (**21**).

^{1}H NMR ($CDCl_3$, δppm): 6.77-6.85 (m, 3H), 4.37-4.40 (d, 2H), 3.80 (s, 3H), 3.77 (s, 3H), 2.03 (s, 3H)

GC-MS: *m/z* (%) = 209 (M^+), 166, 152, 136, 124, 108, 77, 69, 53

2,5-Dihydroxybenzylacetanilide (22)

Synthesis of **22** was carried out as described earlier for **15** using 2,5-dimethoxybenzalacetanilide (10, 0.209 g, 1 mmol) and 1M boron tribromide solution (3.1 ml, 3 mmol) in dichloromethane (60 ml). Overall yield was 52%.

^{1}H NMR ($CDCl_3$, δppm): 6.63-6.93 (m, 3H), 4.21-4.24 (d, 2H), 1.96 (s, 3H)

Methylene-16-crown-5 (3)

A solution of 3-chloro-2-chloromethyl-1-propene (**2**, 2.5 g, 20 mmol) and tetraethylene glycol (**1**,3.88 g, 20 mmol) in THF (30 ml) was added drop wise to a stirred suspension of sodium hydride (1.44 g, 60 mmol) in THF (30 ml) at a reflux temperature under an argon atmosphere. The mixture was kept stirring for additional two hours, filtered. The solvents were evaporated in vacuo to yield 1.60 g (yield 32.5%) of a yellow oil methylene-16-crown-5 (**3**). The product is purified by vacuum distillation (b.p. 190-200°C / 0.3 mmHg).

^{1}H NMR ($CDCl_3$, δppm): 5.17 (s, 1H), 4.17 (s, 2H), 3.67-3.69 (m, 8H)

Oxo-16-crown-5 (4)

A solution of methylene-16-crown-5 (**3**, 0.738 g, 3 mmol) in dichloromethane (20 ml) was cooled to –78°C and ozone was babbled through it at –78 °C until the solution turned blue. To this solution was added dimethyl sulfide (0.558 g, 9 mmol) at –78°C. Then, the mixture was stirred at room temperature for five hours, washed with water and saturated aqueous sodium chloride. The organic layer was dried over magnesium sulfate, concentrated to give 0.632 g (yield 85%) of a colorless oil oxo-16-crown-5 (**4**).

^{1}H NMR ($CDCl_3$, δppm): 4.46 (s, 2H), 3.62 (m, 8H)

^{13}C NMR ($CDCl_3$, δppm): 207.46, 75.64, 71.40, 70.58, 70.42, 70.36

IR ($CHCl_3$): ν = 3053.7, 2877.5, 1735.5, 1272.2, 1128.6

1,4-Dimethoxynaphthylmagnesium bromide (6)

To a solution of 1,4-dimethoxy-2-bromonaphthalene (**5**, 0.335 g, 1.2 mmol) in anhydrous THF (5 ml) was added magnesium powder (0.05 g, 2.08 mmol) and a small piece of iodine. The mixture was kept stirring for one and a half hour to give a gray suspension 1,4-dimethoxynaphthaylmagnesium bromide (**6**).

1-Hydroxy-1-(2',-5'-dimethoxynaphthyl)-16-crown-5 (7)

The suspension from above Grignard procedure 1,4-dimethoxynaphthaylmagnesium bromide (**6**) was cooled to 10 °C. To this solution was added oxo-16-crown-5 (**4**, 0.37 g, 1.2 mmol) and anhydrous THF (5 ml). The mixture was stirred for additional one hour at room temperature. The reaction was quenched by pouring onto ice water. The precipitated magnesium compounds were treated with 10 percent hydrochloric acid. The mixture was extracted by ethyl acetate. The organic layer was washed with water and saturated aqueous sodium chloride, dried over magnesium sulfate, concentrated to yield 0.25 g (yield 48%) of a yellow oil 1-hydroxy-1-(2',-5'-dimethoxynaphthyl)-16-crown-5 (**7**).

^{1}H NMR ($CDCl_3$, δppm): 7.95-8.23 (dd, 2H), 7.41-7.58 (m, 2H), 7.29 (s, 1H), 4.99 (s, 1H), 4.21-4.29 (m, 4H), 3.99 (s, 3H), 3.90 (s, 3H), 3.62-3.78 (m, 16H)

^{13}C NMR ($CDCl_3$, δppm): 130.52, 129.61, 126.65, 125.74, 125.67, 122.89, 122.66, 122.56, 71.33, 71.06, 70.80, 70.43, 63.39, 56.21

1-(2',5'-Dimethoxynaphthyl)-16-crown-5 (8)

The solution of 1-hydroxy-1-(2',-5'-dimethoxynaphthyl)-16-crown-5 (**7**, 0.347 g, 0.8 mmol), lithium aluminum hydride (0.044 g, 1.19 mmol) and aluminum chloride (0.312 g, 2.34 mmol) in anhydrous THF (15 ml) was heated at reflux for twelve hours. The mixture was quenched by cold water and ethyl acetate. The diluted sulphuric acid was added to decompose aluminum complexes. The mixture was extracted by dimethyl ether. The organic layer was washed with water, dried over magnesium sulfate, filtrated, and concentrated to give 0.202 g (yield 60%) of a brown oil 1-(2',5'-dimethoxynaphthyl)-16-crown-5 (**8**).

^{1}H NMR ($CDCl_3$, δppm): 8.05-8.26 (m, 2H), 7.44-7.49 (m, 2H), 6.46 (s, 1H), 3.92 (s, 3H), 3.67 (s, 3H), 3.56-3.84 (m, 21 H)

2-Amino-1,4-naphthoquinone (26)

To a solution of 1,4-naphthoquinone (**25**, 5 g, 31.64 mmol) in glacial acid (50 ml) at 40°C was added a solution of sodium azide (3.4 g, 52.31 mmol) in water (10 ml). Gas was evolved. The mixture was stirred for one and a half hour. On cooling, the brown crystalline material which had separated was collected and washed with water. The crystal was purified by recrystallization from alcohol to yield 4.65 g (yield 85%) of an orange red crystal 2-amino-1,4-naphthoquinone (**26**).

^{1}H NMR ($CDCl_3$, δppm): 8.04-8.09 (m, 2H), 7.63-7.73 (m, 2H), 6.00 (s, 1H), 5.21 (br, 2 H), 1.64-1.65 (br, 4H)

GC-MS: *m/z* (%) = 173 (M^+), 146, 117, 105, 89, 76, 68, 50

2-amino-1,4-naphthoquinone hydrochloride (27)

2-amino-1,4-naphthoquinone (**26**, 0.311 g, 1.8 mmol), methanol (10 ml), water (5 ml) and 3M hydrochloric acid (5 ml) in a 50-ml round-bottomed flask were heated at reflux under argon atmosphere for five hours. After cooling the mixture, the solvents were removed in vacuo to give 0.30 g (yield 80%) of a brown yellow powder 2-amino-1,4-naphthoquinone hydrochloride (**27**).

^{1}H NMR ($CDCl_3$, δppm): 7.75-8.02 (m, 4H), 6.19 (s, 1H)

GC-MS: *m/z* (%) = 174 (M^+), 146, 105, 89, 77, 50

Sodium picrate (28)

To a solution of picric acid (0.46 g, 2 mmol) in ethanol (10 ml) was added a solution of sodium hydroxide (0.2 g, 5 mmol) in ethanol (10 ml) drop wise. After adding, the mixture was cooled over ice, the brown red crystal which had separated was collected and washed with ice water to yield 0.20 g (yield 40%) of a brown red crystal sodium picrate (**28**). The product was dried in dark.

Potassium picrate (29)

To a solution of picrate acid (0.46 g , 2 mmol) in water (40 ml) was added a solution of potassium hydroxide (0.336 g, 6 mmol) in water (1.2 ml). The mixture was stirred for half an hour. The yellow crystalline material which had separated was collected and washed with ice water to yield 0.454 g (yield 80%) of a yellow crystal potassium picrate (**29**). The product was dried in dark.

Cesium picrate (30)

The synthesis of cesium picrate was carried out as the same method for above potassium picrate (**29**) using cesium hydroxide hydrate (0.504 g, 3 mmol) and picric acid (0.23 g, 1 mmol).

Rubidium picrate (31)

The synthesis of rubidium picrate was carried out as the same method for above potassium picrate (**29**) using rubidium hydroxide hydrate (0.36 g, 3 mmol) and picric acid (0.23 g, 1 mmol).

Dimethoxybenzene ammonium picrate (32)

To a solution of picric acid (0.227 g, 0.99 mmol) in as less as possible water was added a solution of dimethoxyaniline hydrochloride (0.15 g, 0.79 mmol) in as less as possible water. After adding, the mixture was kept stirring for additional half an hour. The yellow crystalline material was collected to give 0.24 g (yield 65%) dimethoxybenzene ammonium picrate (**32**). The product was dried in dark.

^{1}H NMR (acetone-d^{6}, δppm): 8.72 (s, 1H), 7.04-7.26 (m, 2H), 3.79 (s, 3H), 3.86 (s, 3H)

General method to determine the association constant (Ka) by the Ultraviolet Method:

Picrate salts in distilled water in volumetric flask (200 ml) were prepared that involved the following cations (concentrations): Li^{+} (0.015 M); Na^{+} (0.015 M); K^{+} (0.015 M); Rb^{+} (0.010 M); Cs^{+} (0.010 M); NH_4^{+} (0.015 M). Solutions of the host, 0.075 M in $CHCl_3$, were also prepared in either 1.00 or 2.00 ml volumetric flasks.

Into a 12-ml centrifuge tube was introduced a measured volume of picrate solution. The volume for rubidium and cesium picrates was 1.0 ml; for all others it was 0.5 ml. A small magnetic stir bar was then added to the tube. To one tube was added 1.0 ml of water to be used as a blank. To each of the tubes, including the one containing water, was added 0.2 ml of the host solution. The tubes were stoppered to prevent evaporation and briefly centrifuged to cause the $CHCl_3$ layer to sink. The contents of each tube were then stirred vigorously for three minutes by means of a magnetic stir placed on inside, and separated into two clear layers by centrifugation.

An aliquot of the $CHCl_3$ layer was measured and transferred by micro syringe into a 5-ml volumetric flask and diluted to the mark with acetonitrile. With more intensely colored layers, only 0.01 ml aliquot was used; with less intensely colored layers, 0.05 ml aliquots were used. For each size of aliquot, a blank was also made by measuring the desired volume from $CHCl_3$ layer of the water blank and diluting to the mark with acetonitrile in a 5-ml volumetric flask. The UV

absorption of each 5-ml solution was measured against the appropriate blank solution at 380 nm. The same cell was always used for the unknown, and their orientation in the spectrophotometer was always kept same.

Calculations were based on the Beer's law relationship, $a = \varepsilon bc$, where a is the absorbance, ε the extinction coefficient, b the path length of the cell, and c the concentration of the measured species. The total millimoles of picrate salt in the measured aliquot were equal to the product of c and the volume of the measured solution, which was 5 ml. The millimole of host was the product of the host concentration and the aliquot volume. The guest to host molar ratio, R, which was the same in the measured aliquot as in the original $CHCl_3$ layer, was given by the millimole of picrate salt divided by the millimole of host.

The distribution constant (K_d) of the alkali and ammonium picrates between water and chloroform were determined as follows. Picrate solutions of known concentrations in 200 ml of distilled water were shaken in a sealed separatory funnel with 300 ml ethanol-free chloroform. The layer was allowed to separate and clarify about fourteen hours, and the lower layer was very carefully transferred through the stopcock to a flask where the solvent was evaporated on a rotary evaporator under vacuum. The residue was quantitatively transferred with acetonitrile to a 5.00-ml volumetric flask and diluted with acetonitrile to the mark. By the above UV techniques, the amount of picrate salt extracted was calculated.

IV. References

(1). Paddon-Row, M.N. *Acc. Chem. Res.* 1994, **27**, 18

(2). Deisenhofer, J.; Michel, H. *Angew. Chem. , Int. Ed. Engl.* 1989, **28**, 829

(3). Deisenhofer, J.; Epp, O.; Miki, K.; Huber, R. Michel, H. J. *J. Mol. Biol*. 1984, **180**, 385

(4). Norris, J. R.; Gast, P. *J. Photochem.* 1985, **29**, 185.

(5). Wasieleski, M.R. *Chem. Rev*. 1992, **92**, 435

(6). Calcaterr, L.T.; Closs, G.L.; Miller, J.R. *J. Am. Chem. Soc.* 1983, **105**, 670

(7). Khundkar, L.R.; Perry, J.W.; Dervan, P.B. *J. Am. Chem. Soc.* 1994, **116**, 9700

(8). Gray, H.B.; Winkler, J.R. *Annu. Rev. Biochem.* 1996, **65**, 537

(9). McLendon, G.; Hake, R. *Chem. Rev.* 1992, **92**, 481

(10). McConnell, H. M. *J. Chem. Phys*. 1961, **35**, 308

(11) Bertz, J. V.; Miller, J.R. *J. Chem. Phys*. 1979, **71**, 4579

(12). Ward, M.D. *Chem. Soc. Rev.* 1997, **26**, 365

(13). Kirby, J.D.; Roberts, J.A.; Nocera, D.G. *J. Am. Chem. Soc*. 1992, **114**, 4013

(14). de Rege, P.J.F.; Williams, S.A.; Therien, M.J. *Science* 1995, **269**, 1409

(15).Onuchic, J.N.; Beratan, D. N. *J. Chem. Phys*. 1990, **92**, 722

(16). Marcus, R.A. *J.Chem. Phys.* 1956, **24**, 966

(17). Marcus, R.A. *J. Chem. Phys.* 1965, **43**, 679

(18). Hug, G.L.; Marciniak, B. *J. Phys. Chem.* 1995, **99**,1478

(19). Efrima, S.; Bixon, M. *Chem. Phys. Lett*. 1974, **25**,34

(20). Ohno, T.; Yoshimura, A.; Shioyama, H.; Mataga, N. *J. Phys. Chem*. 1987, **91**, 4365

(21). Gould, I.R.; Ege, S.; Mattes, S.L.; Farid, S. *J. Am. Chem. Soc*. 1987, **109**, 3794

(22). Kuznetsov, A.M.; Ulstrup, J. *J.Chem. Phys.* 1981, **75**, 2074

(23). Larsson, S. *J.Am. Chem. Soc.* 1981, **103**, 4034

(24). Beratan, D.N.; Hopfield, J.J. *J. Am. Chem.Soc.* 1984, **106**, 1584

(25). Forster, TH. *Ann. Phys.* **2**: 55-75

(26). Winkler, J.R.; Gray, H.B. *Chem. Rev*. 1992, **92**, 369

(27). Schanze, K.S.; Cabana, I.A. *J. Phys. Chem*. 1990, **94**, 2740

(28). Closs, G.L.; Miller, J.R. *Science* 1988, **240**, 440

(29). Perkins, T.A.; Hauser, B.T.; Eyler, J.R.; Schanze, K.S. *J.Phys. Chem.* 1990, **94**, 8745

(30). Joran, A.D.; Leland, B.A.; Geller, G.G.; Hopfield, J.J.; Dervan, P.B., *J. Am. Chem. Soc.* 1984, **106**, 6090

(31). Stein, C.A.; Lewis, N.A.; Seitz, G. *J. Am. Chem. Soc.* 1982, **104**, 12596

(32). Hush, N.S.; Paddon-Row, M.N. *Chem. Phys. Lett.* 1985, **117**,8

(33). Zimmerman, H.E., Makelvey, R.D. *J. Am. Chem. Soc.* 1971, **93**, 3638

(34). Zimmerman, H.E.,Goldman, T.D., Hirzel, T.K., Schmidt, S.P. *J. Org. Chem*. 1980, **45**, 3933

(35). Beecroft, R.A.; Davidson, R.S.; Goodwinn, D.; Pratt, J.E. *Pure App. Chem*. 1982, **54**, 1605

(36). Cram, D.J. *Angew. Chem. Int. Ed. Engl.* 1986, **25**, 1039

(37). Timko, J.M.; Moore, S.S.; Walba, D.M.; Hiberty, P.C.; Cram, D.J. *J. Am. Chem. Soc.* 1977, **99**, 4207

(38). Tomoi, M.; Abe, O.; Ikeda, M.; Kihara,K.; Kakiuchi, H. *Tetrahedron Lett.* 1978, 3031

(39). Kauer, J.C. *Am. Chem. Soc*. 1970, **15**, B14

(40). Beak, P.; Kokko, B.J. *J.Org. Chem.* 1982, **47**, 2822

(41). Brewester, J.H.; Osman, S.F.; Bayer, H.O.; Hopps, H.B. *J. Org. Chem*. 1964, **29**, 121

(42). Heene, A.L.; Hill, P. *J. Am. Chem. Soc*. 1943, **65**, 752

(43). Lin, C.C.; Wu, H.J. *Synthesis* 1996, 715

(44). Herbert, E,; Karl, T.Z. *J. Org. Chem.* 1951, **16**, 64

(45). Cason, J. *Org. Reactions*, Vol. IV. 1948, John Wiely & Sons Inc.

(46). Fiesher, L.F.; Jonathan, H.L. *Am. Soc*. 1935, **57**, 1482

(47). Lansinger, J.M.; Ronald, R.C. *Synthetic Communication* 1979, **9**, 341

(48). Cram, D. *J. Angew. Chem. Int. Ed. Engl.* 1986, **25**, 1039

(49). Beresford, G.D.; Stoddart, J.F. *Tetrahedron Lett.* 1980, **21**, 867

(50). Timko, J.M.; Moore, S.S.; Walba, D.M.; Hiberty, P; Cram, D.J. *J. Am. Chem. Soc.* 1977, **99**, 4207